

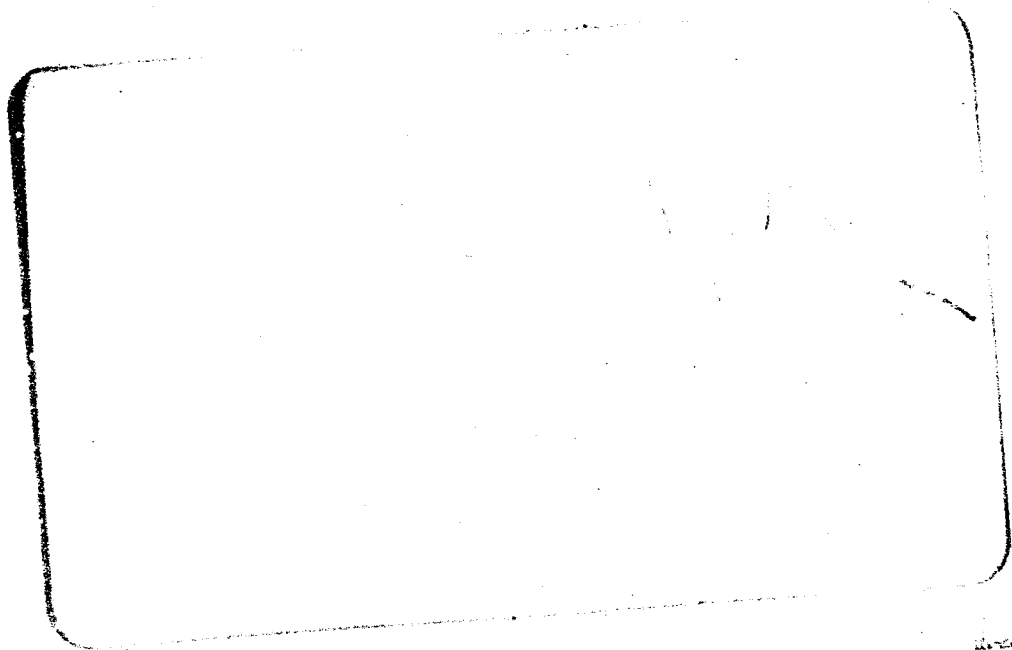
AR-002-715

AD-A149 826

THE UNITED STATES NATIONAL  
TECHNICAL INFORMATION SERVICE  
IS AUTHORIZED TO  
REPRODUCE AND SELL THIS REPORT



AUSTRALIAN ARMY



DTIC FILE COPY

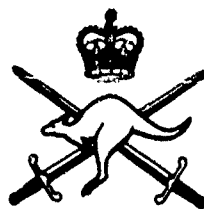
APPROVED  
FOR PUBLIC RELEASE

DTIC  
ELECTE  
JAN 29 1985

A

BEST  
AVAILABLE COPY

85 01 22 030



# AUSTRALIAN ARMY



## ENGINEERING DEVELOPMENT ESTABLISHMENT

SKID STEERING OF WHEELED AND  
TRACKED VEHICLES - ANALYSIS WITH  
COULOMB FRICTION ASSUMPTIONS

BY

A.P. CREEDY

PUBLICATION EDE 38/84

Prepared and issued under my direction.

*P.J.A. Evans*  
(P.J.A. Evans)  
Brigadier  
Commander

DTIC  
SELECTED  
JAN 29 1985  
A

MARIBYRNONG VICTORIA

PRIVATE BAG 12,  
PO ASCOT VALE,  
VICTORIA 3022.

Victoria

Distribution: Approved for Public Release  
Neg. No. 8585

© COMMONWEALTH OF AUSTRALIA

DISTRIBUTION

<u>Addressee</u>	<u>No of Copies</u>
<u>Army Office</u>	
CMAT	1
DVP	1
<u>Defence Central</u>	
J10 (DDSTI)	1
<u>Defence Science and Technology Organization</u>	
CDS	1
SA-A	1
ARL	1
DRCS	1
MRL	1
DISB (Document Exchange Centre)	18
<u>Libraries</u>	
Defence Central (Technical Reports Centre)	1
Defence Regional Victoria	1
ARL	1
MRL	1
DRCS	1
<u>Internal</u>	
COMD	1
SME	1
ME(AFV)	1
S&P	1
Library	1
Author	1
File	1
Spare	2
Total	<u>40</u>

100

CONTENTS

	<u>Page No</u>
DISTRIBUTION	ii
SUMMARY	iii
CONTENTS	iv-v
GLOSSARY	viii-xi
REFERENCES	1
 List of Annexes	
	<u>Para No</u>
INTRODUCTION	1
AIM	5
BASIC PRINCIPLES AND ASSUMPTIONS	
Limitations of Theory	6
Instantaneous Centres of Rotation	11
Radius of Turn	15
Slip Velocities and Steering Ratio	18
Slope Operation	22
DETERMINATION OF INSTANTANEOUS CENTRE OF ROTATION (ICR) FOR EACH ROW OF WHEELS, OR TRACK, RELATIVE TO THE GROUND	
Forces Acting at Wheel/Ground Contact Points	23
Vehicle Equilibrium	32
DERIVATION OF INDIVIDUAL WHEELS LOADS	40
EFFECT OF SUSPENSION AND FINAL DRIVE ARRANGEMENT ON WHEEL LOADS	
Wheeled Vehicle	58
Tracked Vehicle	67
CALCULATION OF POWER INPUT AND DISSIPATION	
Wheeled Vehicle	72
Tracked Vehicle	74
OVERALL METHOD OF COMPUTATION	75

	v	
PARTICULARS OF VEHICLES		78
TV1000		
General		79
Leading Dimensions and Weight		80
Suspension Characteristics		81
Radius Arm Geometry		84
Friction Coefficients		87
Rolling Resistance		88
Tyre Contact Point Movement		89
TV1333		
General		92
Leading Dimensions and Weight		93
Suspension Characteristics		96
Radius Arm Geometry		97
Friction Coefficients		98
Rolling Resistance		99
Tyre Contact Point Movement		100
TV6000		
General		101
Leading Dimensions and Weight		102
Suspension Characteristics		103
Radius Arm Geometry		104
Friction Coefficients		105
Rolling Resistance		106
Tyre Contact Point Movement		107
RESULTS OF SKID STEERING CALCULATIONS		
TV1000 - Torque Input to Individual Wheels		108
Variation of Steering Ratio, Power Input and Power		
Dissipation with Radius of Turn		111
Steering on Slopes		116
CONCLUSIONS		124
RECOMMENDATIONS		129

LIST OF ILLUSTRATIONS  
(Contained in Annex D)

<u>Fig No</u>	<u>Title</u>
1	External Forces Acting on a N X N Skid Steered Wheeled Vehicle in a Constant Rate Turn
2	N Wheeled Skid Steered Vehicle - Coordinate System for Wheel/Ground Contact Points and Instantaneous Centres of Rotation (ICR) for Each Row of Wheels
3	Typical ICR Positions and Inertia Forces Acting at Vehicle C of G
4	Velocities of Tracks Relative to Hull
5	Velocities of Tracks Relative to Hull
6	Operation of Vehicle on Slope - Resolution of Weight
7	Suspension Deflections and Chassis Attitude Resulting from Forces Acting at Vehicle C of G
8	Forces and Torques Acting on Individual Wheels and Suspension Radius Arms
9	Tracked Vehicle - Track Forces $F_3(j)$ and Resulting Forces at Wheels
10	Overall Method of Computation
11	TV1000 - Assumed Suspension Force/Deflection Characteristic
12	TV1000 - Estimation of Wheel/Ground Contact Point Movement
13	TV6000TR - Assumed Suspension Force/Deflection Characteristic
14	TV1333 - Variation of Steering Ratio with Radius of Turn for Various Forward Speeds
15	TV6000TR - Variation of Steering Ratio with Radius of Turn for Various Forward Speeds
16	TV6000TR - Variation of Power Input and Dissipation with Radius of Turn at 20 Ft/s Forward Speed
17	TV1000 - Variation of Power Input and Dissipation with Radius of Turn at 20 Ft/s Forward Speed
18	TV1333 - Variation of Power Input and Dissipation with Radius of Turn at 20 Ft/s Forward Speed
19	TV1000 - Variation of Specific Coordinates of ICR with Heading Angle at a Fixed Slope Angle
20	TV1000 - Slope Steerability Diagram

- 21 TV1000 - Variation of Steering Ratio with Radius of Turn at Negligible Forward Speed
- 22 TV1333 - Slope Steerability Diagram
- 23 TV6000TR - Slope Steerability Diagram
- 24 TV1000 - Variation of Steering Ratio with Radius of Turn for Various Forward Speeds



GLOSSARY - PRINCIPAL USE OF SYMBOLS

A(J) (J = 1,2)	Non dimensional lateral (measured at right angles to vehicle centreline) coordinates of track ICRs relative to ground.
B	Non dimensional longitudinal (measured along vehicle centreline) coordinate of track ICRs relative to ground.
C(J) (J = 1,2)	Lateral coordinates of wheel/ground contact points, measured from vehicle centreline.
C(3)	Lateral coordinate of CG measured from vehicle centreline.
D4(I) (I = 1,N)	Deflection of suspension of Ith wheel from position at which zero force $W_1(I)$ is developed.
D6	Suspension deflection when radius arm angle is $T_7$ .
D7	Longitudinal component of vehicle weight acting through CG.
D8	Longitudinal inertia force acting through CG.
D9	Sum of D7 and D8.
D0	Deflection of origin of chassis coordinate system from a position corresponding to zero deflection of each wheel suspension.
F1(I) (I = 1,N)	Longitudinal forces generated at the Ith wheel/ground contact point.
F3(J) (J = 1,N)	Track tension (tracked vehicles only).
F(J) (I = 1,N)	Longitudinal forces generated during sliding by entire 'row' of wheel/ground contact point.
G8	Slope heading angle.
G9	Roll angle of chassis, relative to ground.
H	Height of CG above ground.
I	Subscript used to label properties associated with the Ith wheel of an N-wheeled vehicle.
J	Subscript used to label properties associated with the left (J = 1) or right (J = 2) side of the vehicle.
K	Subscript used to label properties associated with the Kth pair of wheels of an N-wheeled vehicle, K = 1 denoting the front wheels.
K1(K)	Suspension deflection due to adjustment of suspension medium away from nominal position.

GLOSSARY - PRINCIPAL USE OF SYMBOLS

A(J) (J = 1,2)	Non dimensional lateral (measured at right angles to vehicle centreline) coordinates of track ICRs relative to ground.
B	Non dimensional longitudinal (measured along vehicle centreline) coordinate of track ICRs relative to ground.
C(J) (J = 1,2)	Lateral coordinates of wheel/ground contact points, measured from vehicle centreline.
C(3)	Lateral coordinate of CG measured from vehicle centreline.
D4(I) (I = 1,N)	Deflection of suspension of Ith wheel from position at which zero force $W_1(I)$ is developed.
D6	Suspension deflection when radius arm angle is $T_7$ .
D7	Longitudinal component of vehicle weight acting through CG.
D8	Longitudinal inertia force acting through CG.
D9	Sum of D7 and D8.
D0	Deflection of origin of chassis coordinate system from a position corresponding to zero deflection of each wheel suspension.
F1(I) (I = 1,N)	Longitudinal forces generated at the Ith wheel/ground contact point.
F3(J) (J = 1,N)	Track tension (tracked vehicles only).
F(J) (I = 1,N)	Longitudinal forces generated during sliding by entire 'row' of wheel/ground contact point.
G8	Slope heading angle.
G9	Roll angle of chassis, relative to ground.
H	Height of CG above ground.
I	Subscript used to label properties associated with the Ith wheel of an N-wheeled vehicle.
J	Subscript used to label properties associated with the left (J = 1) or right (J = 2) side of the vehicle.
K	Subscript used to label properties associated with the Kth pair of wheels of an N-wheeled vehicle, K = 1 denoting the front wheels.
K1(K)	Suspension deflection due to adjustment of suspension medium away from nominal position.

K <sub>1</sub>	Rolling resistance proportionality constant.
K <sub>2</sub>	Indicator for direction of rolling resistance forces. $K = -1$ corresponds to positive (forward) rolling resistance force, $K = +1$ to negative rolling resistance force.
K <sub>4</sub>	Tyre contact patch movement proportionality constant, as defined in equation (4-3).
I <sub>1</sub>	Track approach angle.
I <sub>2</sub>	Track departure angle.
L(K)	Longitudinal coordinates of wheel/ground contact points. $L(N/2 + 1)$ is CG coordinate.
M(3)	Movement generated by longitudinal and lateral forces acting through vehicle CG.
M <sub>8</sub>	Coefficient of friction in transverse, or lateral, direction.
M <sub>9</sub>	Coefficient of friction in longitudinal direction.
M(J) (J = 1,2)	Sums of moments of lateral skid steering forces as defined by equation (2-8).
M <sub>0</sub>	Sum of moments of forces applied externally upon vehicle, about lateral centreline, as defined by equation (3-5).
N	Total number of wheel/ground contact points associated with a vehicle.
N <sub>4</sub>	Power dissipated in longitudinal sliding of wheel/ground contact points.
N <sub>5</sub>	Power dissipated in lateral sliding of wheel/ground contact points.
N <sub>6</sub>	Power input to wheels assuming 100% transmission and regenerative efficiency.
P <sub>1</sub> (I) (I = 1,N)	Transverse force generated at the Ith wheel/ground contact point as a result of transverse sliding.
R	Radius of turn, measured at CG.
R <sub>2</sub>	Distance between centre of turn and vehicle centreline.
R <sub>6</sub> (I)	Motion resistance forces generated at the Ith wheel/ground contact point.
R <sub>8</sub>	Output/Input rotational speed ratio of driveline components enclosed within radius arm.
R <sub>9</sub>	Distance between centre of rotation of radius arm and centre of rotation of attached wheel.

x

S Steering ratio  $V1(1)/V1(2)$ .

S(D4(I)) Functional relationship between suspension deflection D4(I) and suspension force W1(I) at the Ith wheel station.

T Sum of T4 and T5.

T2(I) Torque applied to Ith wheel.

T4 Transverse component of vehicle weight, acting through vehicle CG.

T5 Transverse inertia force acting through vehicle CG.

T6 Yaw angle - angle between vehicle centreline and direction of motion of CG.

T7 Radius arm angle when suspension deflection is D6.

T8(I) Angle of Ith radius arm with respect to datum on chassis.

T9 Chassis roll angle.

V Velocity of vehicle measured at CG.

V1(I)  
(J = 1,2) Velocities of each 'track' or row of wheel/ground contact points relative to the vehicle.

V2(J)  
(J = 1,2) Velocities of each 'track' relative to the ground, resolved parallel to the longitudinal centreline of the vehicle, or slip velocities.

V3(J)  
(J = 1,2) Velocities of the vehicle hull at the track attachment points, resolved parallel to the longitudinal centreline of the vehicle.

V0 Velocity of vehicle measured along vehicle centreline.

W(I) Vertically upward force applied at the Ith wheel/ground contact point.

W1(I) Vertically downward force applied by the suspension at the Ith wheel/ground contact point.

W2(I) Vertically downward force applied at the Ith wheel/ground contact points as a result of the generation of propulsive and skid steering forces.

W3 Vertical component of vehicle weight acting through CG.

W4 Vehicle weight, acting through CG.

W9 Wheel diameter.

x Tyre contact patch movement in a forward direction, due to torque transmitted to wheel.

xi

$Z(K)$  Indicator for direction of radius arms on wheeled vehicle  
( $K = 1, N/2$ )  $Z(K) = -1$  denotes 'leading' radius arm,  $Z(K) = +1$  denotes  
trailing radius arm.

ENGINEERING DEVELOPMENT ESTABLISHMENT  
SKID STEERING OF WHEELED AND TRACKED VEHICLES -  
ANALYSIS WITH COULOMB FRICTION ASSUMPTIONS  
(TASK ARM 82/008)

by

A.P. CREEDY

REFERENCES

- A. Skid Steering by K.R. Weiss  
(Automobile Engineer April 1971)
- B. A Theoretical Analysis of Steerability of Tracked Vehicles  
by M. Kitano and H. Jyozaki
- C. Tracked Vehicles. An Analysis of the Factors Involved in  
Steering by W. Steeds  
(Automobile Engineer, April 1950)
- D. The Performance of a Large-Wheeled Skid-Steered Vehicle.  
An Interim Report on the Operations of TV1000.  
FVRDE Report No BR 189 dated 1 June 1966.

INTRODUCTION

1. Skid steering has been widely applied to track laying vehicles such as bulldozers and current main battle tanks. Tracks are insufficiently flexible in a lateral direction to permit them to be laid on the ground in curves corresponding to a practical radii of turn. Instead, the propulsive force applied by one track is increased relative to the other until the vehicle is forced to slew in the desired direction. Basic theory for skid steering of tracked vehicles has been published (Ref C) and introduces analysis of the forces acting upon the track during skid steering.

2. In military track laying vehicles, the use of skid steering has a useful byproduct in that the tracks and suspension do not consume a large proportion of the internal volume of the vehicle. Wheeled vehicles have certain inherent advantages, automotively, over 'equivalent' tracked vehicles including the ability to travel fast over smooth ground for a relatively lower power input. Wheeled and tracked vehicles have both advantages and disadvantages in particular applications but it is not the aim of this document to examine all of these. A wheeled vehicle may well be a viable competitor to a tracked vehicle for a particular application, and pressure to maximise use of internal volume, together with other considerations, can result in consideration of a skid steered wheeled concept.

3. Skid steering of a wheeled vehicle can be achieved by increasing the total torque driving the row of wheels on one side of the vehicle relative to the torque supplied to the other row of wheels, until the vehicle is forced to slew. During skid steering, the rotational speed of the wheels in one line or row will increase relative to the other row, but normally the transmission arrangement imposes equal rotational speed on all wheels within a row.

4. Theory applying to skid steering of wheeled vehicles has been published (Ref A). Few skid steered wheeled military vehicles have been built to date, and data on their steering performance is insufficient for making informed comparisons with existing vehicles.

### AIM

5. The aim of the work documented here was to make use of skid steering theory to predict the steering characteristics of wheeled skid vehicles, and to compare these with the steering characteristics of tracked vehicles predicted by similar theory. Where possible, the results of theoretical predictions are compared also with experimental data.

### BASIC PRINCIPLES AND ASSUMPTIONS

#### Limitations of Theory

6. The existing theory (Ref A) for wheeled vehicles has the following limitations:

- a. Vehicle motion on flat hard ground at constant speed only is considered.
- b. Wheels are laterally and longitudinally rigid, and contact the ground at a single point. Forces generated by sliding of these points relative to the ground is governed by coulomb friction laws.
- c. Lateral and longitudinal forces may be applied at the vehicle CG, but lateral forces only are considered when calculating the vertical load carried by each row of wheels. Equal vertical loads are assumed to be carried by each wheel within a row.
- d. The effects of the following upon the vertical load carried by each wheel are not considered:
  - (1) Suspension flexibility.
  - (2) Vertical forces generated at each wheel which are a function of torque transmitted, and the specific driveline and suspension arrangement.
- e. The theory deals with a 6 wheel vehicle with symmetrical wheel spacing and CG position fixed in a horizontal plane

7. The theory has been extended within this document and attempts to overcome the last three limitations at c, d and e above, by considering an N-wheeled vehicle (N may be set to 4 or any greater number divisible by 2) where effects on individual wheel loads due to wheel suspension characteristics, variable positioning of the CG in three dimensions, forces applied at the CG, unequal wheel spacing, and vertical forces caused by torque transmitted to each wheel are calculated. The longitudinal flexibility of the tyres is partially considered by application of rolling resistance forces at each wheel, proportional to the load carried, and by introducing a longitudinal movement of the wheel/ground contact point proportional to the torque being applied to the wheel.

8. The theory developed in this document does not deal with the most significant of the limitations, a and b above, the non applicability to motion on soft ground, and the overall effects of tyre flexibility. These limitations remain for future resolution.

9. As detailed within this document, the theory as developed can be applied to tracked vehicles, due allowance being made for the different way in which track tension will modify the fraction of vehicle weight carried by each road wheel. When modified for tracked vehicles, the theory developed here becomes similar to that given in Ref B.

10. Within this document, the symbol I has been used to refer to the Ith wheel, ( $I = 1$  to  $N$ ), J to the Jth row of wheels ( $J = 1, 2$  with 1 referring to the row on the outside of the turn) and K to the Kth "axle" or pair of wheels ( $K = 1, N/2$ ). For given values of J and K,  $I = N/2 * (J-1) + K$ . Where mathematical relationships stated in this document have been used directly in the computer programs used for skid steering calculations, the style of variable name imposed by the BASIC programming language used has, where practicable, been retained.

Note: Throughout this document all figures referenced are figures of Annex D

#### Instantaneous Centres of Rotation

11. Figure 1 shows the essential details of a hypothetical N-wheeled ( $N \times N$ ) vehicle. Wheels within each row are inter connected to run at the same speed. The  $N/2$  points on the underside of the wheels of one row which are in contact with the ground will therefore behave, instantaneously, as a single rigid body, or as a 'track' which is in contact with the ground at  $N/2$  points. The term 'track' is used within this report to denote the  $N/2$  contact points of a row of wheels.

12. Figure 2 shows forces applied to the vehicle in the plane of the wheel/ground contact points, as a result of sliding of the contact points relative to the ground. The vehicle is making a turn to the right, about a point not shown on Fig 2. The left hand 'track', in order to generate forward frictional forces  $F_1$  and lateral forces  $P_1$  as shown sliding rearwards relative to the ground as well as rotating clockwise with the vehicle. Since the 'track' behaves as a rigid body, it rotates about a single point on the ground, in this case  $O_3$  as shown on Fig 2, the Instantaneous Centre of Rotation (ICR) of the 'track' relative to the ground. For the left hand 'track',  $O_3$  is located relative to the vehicle by B and A (1), for the right hand track, the ICR at  $O_2$  is defined by B and



A(2). The actual dimensions of the ICR coordinates are  $A(1)*L(1)$ ,  $A(2)*L(1)$ ,  $B*L(1)$  where  $L(1)$  is a characteristic vehicle dimension.

13. The 'Theorem of Three Centres' (or Kennedy's Theorem) from two dimensional kinematics provides that the relative instantaneous centres of three rigid bodies in relative motion lie on a straight line. Taking these three bodies as the vehicle, the left hand 'track' and the ground, referring now to Fig 3, the ICR of the vehicle relative to the ground is the centre of turn  $O_1$ , the ICR of the 'track' relative to the vehicle is at infinity (since the track does not rotate relative to the vehicle) on a line at right angles to  $WZ$ , therefore the ICR of the 'track' relative to the ground lies on a line between  $O_1$  and infinity, which is at right angles to  $WZ$ . An identical argument applies to the right hand 'track'. Therefore both ICR  $O_2$  and  $O_3$  lie on a line through  $O_1$  which is at right angles to  $WZ$ . The coordinates of  $O_2$  and  $O_3$  in the longitudinal direction are identical, and defined by  $B$ . The lateral coordinates of the ICR of the tracks relative to the ground are defined as shown in Fig 2 and Fig 3 by  $A(1)$  and  $A(2)$ , which are not necessarily equal.

14. The values of  $A(J)$  are defined as positive when associated with positive (sliding rearwards) slip velocity of the wheel/ground contact points. In the case illustrated in Fig 2 and 3,  $A(2)$  has a negative value. Determination of the location of the two 'track' ICRs will establish the direction of sliding of each contact point, and enable each force  $F_1(I)$ ,  $P_1(I)$ , ( $I = 1, N$ ) to be calculated. Calculation of  $A(1)$ ,  $A(2)$  and  $B$  is covered in para 23 to 39.

#### Radius of Turn

15. Figure 3 shows a skid steered vehicle in a steady turn about a centre of turn  $O_1$  such that the CG follows a circular path of radius  $R$ , at peripheral speed  $V$ .  $R$  is defined as the radius of turn, and  $V$  the total speed of the vehicle, and these are normally required as input data for the calculations described.

16.  $V_0$  is the component of vehicle velocity along the longitudinal centreline through  $O$ . Its value is constant at  $V_0$  at all points along the centreline, including the point of intersection of the centreline with the line joining  $O_1$  with the two 'track' ICR  $O_2$  and  $O_3$ .  $V_0$  is defined as the 'forward speed' of the vehicle.

17. The angle between the directions of  $V$  and  $V_0$  is defined on the yaw angle  $T_6$ . The following relationships apply:

$$\begin{aligned} T_6 &= \sin^{-1} ((B*L(1) - L(N/2 + 1))/R) & - (1-1) \\ V_0 &= V * \cos (T_6) & - (1-2) \\ R_2 &= R * \cos (T_6) - C(3) & - (1-3) \end{aligned}$$

The inertia forces acting at the CG are given by:

$$\begin{aligned} D_8 &= W_4 * V^2/(R*g) * \sin (T_6) & - (1-4) \\ T_5 &= W_4 * V^2/(R*g) * \cos (T_6) & - (1-5) \end{aligned}$$

where  $W_4$  is the mass of the vehicle.

### Slip Velocities and Steering Ratio

18. The triangular construction of Fig 4, based upon the line through O1, O2 and O3 which is at right angles to the longitudinal centreline of the vehicle, provides useful relationships between key velocities. The velocities are (for J = 1, 2):

V1(J) - Velocities of 'tracks' relative to the vehicle.

V2(J) - Velocities of 'tracks' relative to the ground resolved parallel to the longitudinal centreline of the vehicle, or slip velocities.

V3(J) - Velocities of the hull at the track attachment points, resolved parallel to the longitudinal centreline of the vehicle.

19. The triangular nature of the construction joining V3(1), V0 and V3(2) will be obvious from consideration of rotation of the vehicle about O1. The case for erection of the velocities V1(1) and V1(2) at O3 and O2 is less obvious. Consider two outriggers of length A(1)\*L(1), one attached to the hull at A, the other attached to the 'track' at A, both initially in the position A-O3. All points in the two outriggers will diverge at velocity V1(1). However, since O3 is the ICR of the 'track' relative to the ground, the extremity of the outrigger attached to the 'track' will be instantaneously at rest above point O3, and the outrigger attached to the hull, rotates with the hull about O1 and its extremity moves away from point O3 with velocity V1(1). A similar argument applies to V1(2). The construction of V2(J) follows from the relationship:

$$V2(J) = V1(J) - V3(J)$$

20. The steering ratio S is defined as the ratio V1(1)/V1(2) and is equal to the ratio of outer/inner wheel rotational speed. From Fig 4:

$$S = (R2 + C(1) + A(1)*L(1))/(R2 + C(2) + A(2)*L(1)) \quad (1-6).$$

$$V1(1) = V0 * (1 + C(1)/R2 + A(1)*L(1)/R2) \quad (1-7).$$

$$V1(2) = V1(1)/S \quad (1-8).$$

$$V2(J) = A(J)*L(J) * (S*V1(2) - V1(2)) / (C2 + A(1)*L(1) - A(2)*L(1)) \quad (1-9).$$

where C2 = C(1) - C(2) = wheel track.

21. Figure 5 shows a small radius turn being generated by a negative steering ratio. A 'pivot' turn is defined here as a turn with S = -1, and provided that A(1) = A(2), this will result in the centre of turn lying on the longitudinal centreline of the vehicle.

### Slope Operation

22. Figure 6 shows the envelope of wheel/ground contact points WXYZ standing on a slope ABCD which is at an angle T3 to the horizontal. The vehicle is pointing in a direction defined by angle C8, measured in plane ABCD. C8 is referred to as the slope heading angle. The vehicle is turning right, or up the slope. The vehicle weight W4 is resolved into a force W3 normal to plane ABCD, and forces T4 and D7 in the lateral and

longitudinal directions of the vehicle, all acting through the vehicle CG. The following relationships apply:

$$\begin{aligned} W3 &= W4 * \cos(T3) & - (1-10) \\ T4 &= W4 * \cos(G8) * \sin(T3) & - (1-11) \\ D7 &= W4 * \sin(G8) * \sin(T3) & - (1-12) \end{aligned}$$

#### DETERMINATION OF INSTANTANEOUS CENTRE OF ROTATION (ICR)

#### FOR EACH ROW OF WHEELS, OR "TRACK", RELATIVE TO THE GROUND

#### Forces Acting at Wheel/Ground Contact Points

23. Figure 2 shows the positions of the wheel/ground contact points of a  $N \times N$  vehicle relative to a  $L$  (length),  $C$  (width) coordinate system having origin  $O$ , and +ive  $L$  and  $C$  in the directions shown. The contact points of the four corner wheels are at  $W, X, Y, Z$  and the coordinates of the  $I$ th contact point is  $L(K), C(J)$ . The contact points are axially symmetrical,  $C(1) = -C(2)$  and  $L(1) = -L(N/2)$ .

24. As shown in para 13, the ICR coordinates for each row of contact points lie on a line at right angles to the vehicle centreline. For consistency with earlier work, the distance of this line from  $O$  is defined as a multiple  $B$  of the vehicle semi length, or  $B * L(1)$ . The distance of each ICR from the relevant row of wheels is defined as a multiple  $A(J)$  of the vehicle semi length or  $A(J) * L(1)$  ( $J = 1, 2$ ).

25. The transverse and longitudinal (forward propulsive) forces generated by the sliding of each wheel/ground contact point about  $O1$  or  $O2$  are  $F1(I)$  and  $P1(I)$  respectively. ( $I = 1$  to  $N$ ). If the vertical load at each contact point is  $W(I)$  and the wheel/ground coefficients of (coulomb) friction in the transverse and longitudinal directions are  $M8$  and  $M9$  respectively, use of Micklethwaite's suggestion (see Ref A and Ref C) leads to the following equations for  $F1$  and  $P1$ . For  $I = 1$  to  $N$ :

$$\begin{aligned} F1(I) &= M8 * W(I) * \cos(\theta(I)) & - (2-1) \\ P1(I) &= -M9 * W(I) * \sin(\theta(I)) & - (2-2) \end{aligned}$$

the negative sign has been introduced in equation (2) in order to make transverse forces acting at the wheel/ground contact points positive when in the direction of the centre of turn, which in this case is the direction  $O1 - O2$ . Forces  $F$  are positive in the direction of motion of the vehicle.

26. The geometry of Fig 2 leads to the following expressions for  $\cos \theta$  and  $\sin \theta$ :

$$\cos \theta(I) = \frac{A(J) * L(1)}{\sqrt{(L(K) - B * L(1))^2 + (A(J) * L(1))^2}} \quad - (2-3)$$

$$\sin \theta(I) = \frac{L(K) - B * L(1)}{\sqrt{(L(K) - B * L(1))^2 + (A(J) * L(1))^2}} \quad - (2-4)$$

Note that for the situation shown in Fig 2, for  $J = 1$  (the 'outside' row of wheels), all  $\cos \theta$  are  $>0$  and  $\sin \theta <0$  for  $K = 2$  to  $N/2$ . For  $J = 2$  (the 'outside' row of wheels), all  $\cos \theta$  are  $<0$  and  $\sin \theta <0$  for

$K = 2$  to  $N/2$ . Forces  $R6(I)$  ( $I = 1$  to  $N$ ) act at each contact point in a direction opposing forward (Parallel to OL) motion of the relevant row of wheel hubs over the ground. Their sum is the "rolling resistance" of the vehicle.

27. In accordance with the sign convention for longitudinal forces given above, the forces  $R6$  as depicted in Fig 1 and 2 are negative. This is consistent with all wheels rolling in a 'forward' direction which is normally the case despite the forward sliding of the inside (right hand) row of contact points. The forces  $R6$  are therefore assumed to oppose the direction of motion of each side of the vehicle hull parallel to OL and further assumed to have a magnitude proportional to the vertical load carried by the wheel such that:

$$R6(I) = -K2 * W(I) \quad (I = 1 \text{ to } N)$$

where  $K2$  is a suitable constant.

28. In the case of a pivot turn (normally the only practical case where hull velocities  $V3(J)$  are of unequal sign) the right hand row of wheels shown in Fig 2 would have positive (forwards) forces  $R6(I)$  ( $I = N/2 + 1$  to  $N$ ) acting at the contact points. Within the computer programs based upon the theory of this report the following expression was used for  $R6$ . For  $I = 1$  to  $N$ :

$$R6(I) = -K2 * K3 * W(I) \quad - (2-5)$$

where  $K3 = +1$  for all conditions except a pivot turn, when  $K3 = -1$  for  $J = 2$  only.

29. If  $F(J)$ ,  $J = 1, 2$  are the total longitudinal forces generated by the outer and inner 'tracks' respectively, and  $P(J)$ ,  $J = 1, 2$  are the transverse forces:

$$F(J) = \sum_{K=1}^{\frac{N}{2}} (F1(I) + R6(I))$$

$$P(J) = \sum_{K=1}^{\frac{N}{2}} P1(I)$$

30. Using equations (2-1) to (2-5) the above expressions can be re-written:

$$F(J) = M8 \sum_{K=1}^{\frac{N}{2}} W(I) * \sin \theta(I) - K2 \sum_{K=1}^{\frac{N}{2}} K3 * W(I) \quad - (2-6)$$

$$P(J) = -M9 \sum_{K=1}^{\frac{N}{2}} W(I) * \cos \theta(I) \quad - (2-7)$$

31. The transverse forces applied at each contact point apply a moment, opposing the turn, to each row of wheels. If  $M(J)$  ( $J = 1, 2$ ) are the moments applied to each row of wheels, and defining positive moments as anticlockwise in the plane of Fig 2, then:

$$M(J) = - \sum_{K=1}^{\frac{N}{2}} P1(I) * L(K)$$

$$M(J) = M9 \sum_{K=1}^{\frac{N}{2}} L(K) * W(I) * \sin \theta (I) \quad - (2-8)$$

#### Vehicle Equilibrium

32. Figure 2 shows all forces acting in the plane of the ground upon the vehicle at the wheel/ground contact points. Fig 1 is an isometric view of the simplified vehicle considered by this analysis, in which all externally acting forces, including those of Fig 2, are shown.

The additional forces are:

D9 - A rearward longitudinal force acting through the vehicle CG. In a steady turn as considered by this analysis, this will normally be the sum of an inertia force (D8) opposing acceleration of the CG in the forward direction and a component of vehicle weight (D7) acting in a rearward direction, due to the vehicle standing on a slope.

T - A lateral (or transverse) force acting through the vehicle CG. It is the sum of an inertia force (T5) and component of vehicle weight (T4) acting in parallel to OC, away from the centre of turn.

W3 - A component of vehicle weight (W4) acting normally to the plane of the ground (WXYZ).

33. The additional forces D9, T, W3 are positive in the directions shown on Fig 1. If the CG of the vehicle is offset from 00" (Fig 1) by  $L(N+1)$ ,  $C(3)$  measured in the L, C coordinate system, forces T and D9 will generate a moment  $M(3)$  about 00" as follows:

$$M(3) = D9 * C(3) + T * L(N/2 + 1) \quad - (2-9)$$

34. In a turn of constant vehicle speed and radius, the forces shown on Fig 1 will be in equilibrium. Three equations defining this equilibrium are:

(Equilibrium of moments about 00")

$$M(1) + M(2) + M(3) - (F(1) * C(1) + F(2) * C(2)) = 0 \quad - (2-10)$$

(Equilibrium of longitudinal forces)

$$F(1) + F(2) - D9 = 0 \quad - (2-11)$$

(Equilibrium of lateral forces)

$$P(1) + P(2) - T = 0 \quad - (2-12)$$

where M, F and P are defined by equations (2-6), (2-7), (2-8), (2-9).

35. It is required to solve (2-10), (2-11), (2-12) for A(1), A(2) and B for given values of L(K), C(J), W(I), M8, M9 and K2. A numerical method as follows has been found to give single solutions for A(1), A(2), B.

36. For given conditions as stated, the left hand side of equations (2-10), (2-11), (2-12) are treated as functions of A(1), A(2) and B only. Denoting these functions as P2, G2, R2 respectively, if (A(1))<sub>1</sub>, (A(2))<sub>1</sub> and (B)<sub>1</sub> are approximate (guessed) solutions, and subject to errors ΔA(1), ΔA(2), ΔB, then:

$$P2 ((A(1))_1 + \Delta A(1)), ((A(2))_1 + \Delta A(2)), ((B)_1 + \Delta B) = 0 \quad - (2-13)$$

$$G2 ( \quad " \quad " \quad " \quad " \quad " ) = 0 \quad - (2-14)$$

$$R2 ( \quad " \quad " \quad " \quad " \quad " ) = 0 \quad - (2-15)$$

37. Expressing the left hand sides of 13, 14, 15 as the first terms of the Taylor series of P2, G2 and R2 gives:

$$(P2)_1 + \Delta A(1) \left[ \frac{\partial P2}{\partial A(1)} \right]_1 + \Delta A(2) \left[ \frac{\partial P2}{\partial A(2)} \right]_1 + \Delta B \left[ \frac{\partial P2}{\partial B} \right]_1 = 0 \quad - (2-16)$$

$$(G2)_1 + \Delta A(1) \left[ \frac{\partial G2}{\partial A(1)} \right]_1 + \Delta A(2) \left[ \frac{\partial G2}{\partial A(2)} \right]_1 + \Delta B \left[ \frac{\partial G2}{\partial B} \right]_1 = 0 \quad - (2-17)$$

$$(R2)_1 + \Delta A(1) \left[ \frac{\partial R2}{\partial A(1)} \right]_1 + \Delta A(2) \left[ \frac{\partial R2}{\partial A(2)} \right]_1 + \Delta B \left[ \frac{\partial R2}{\partial B} \right]_1 = 0 \quad - (2-18)$$

Suffix 1 denotes evaluation of the relevant function at the points (A(1))<sub>1</sub>, (A(2))<sub>1</sub>, (B)<sub>1</sub>.

38. By treating approximations (2-16), (2-17), (2-18) as equalities, the errors ΔA(1), ΔA(2), ΔB become approximate errors and can be found by solving (2-16), (2-17), (2-18) using standard methods for simultaneous linear equations.

Hence:

$$\Delta A(1) = D1/D$$

$$\Delta A(2) = D2/D$$

$$\Delta B = D3/D$$

$$\begin{aligned}
 \text{where } D &= \begin{vmatrix} \left[ \frac{\partial P_2}{\partial A(1)} \right]_1 & \left[ \frac{\partial P_2}{\partial A(2)} \right]_1 & \left[ \frac{\partial P_2}{\partial B} \right]_1 \\ \left[ \frac{\partial G_2}{\partial A(1)} \right]_1 & \left[ \frac{\partial G_2}{\partial A(2)} \right]_1 & \left[ \frac{\partial G_2}{\partial B} \right]_1 \\ \left[ \frac{\partial R_2}{\partial A(1)} \right]_1 & \left[ \frac{\partial R_2}{\partial A(2)} \right]_1 & \left[ \frac{\partial R_2}{\partial B} \right]_1 \end{vmatrix} \\
 D_1 &= \begin{vmatrix} - (P_2)_1 & \left[ \frac{\partial P_2}{\partial A(2)} \right]_1 & \left[ \frac{\partial P_2}{\partial B} \right]_1 \\ - (G_2)_1 & \left[ \frac{\partial G_2}{\partial A(2)} \right]_1 & \left[ \frac{\partial G_2}{\partial B} \right]_1 \\ - (R_2)_1 & \left[ \frac{\partial R_2}{\partial A(2)} \right]_1 & \left[ \frac{\partial R_2}{\partial B} \right]_1 \end{vmatrix} \\
 D_2 &= \begin{vmatrix} \left[ \frac{\partial P_2}{\partial A(1)} \right]_1 & - (P_2)_1 & \left[ \frac{\partial P_2}{\partial B} \right]_1 \\ \left[ \frac{\partial G_2}{\partial A(1)} \right]_1 & - (G_2)_1 & \left[ \frac{\partial G_2}{\partial B} \right]_1 \\ \left[ \frac{\partial R_2}{\partial A(1)} \right]_1 & - (R_2)_1 & \left[ \frac{\partial R_2}{\partial B} \right]_1 \end{vmatrix} \\
 D_3 &= \begin{vmatrix} \left[ \frac{\partial P_2}{\partial A(1)} \right]_1 & \left[ \frac{\partial P_2}{\partial A(2)} \right]_1 & - (P_2)_1 \\ \left[ \frac{\partial G_2}{\partial A(1)} \right]_1 & \left[ \frac{\partial G_2}{\partial A(2)} \right]_1 & - (G_2)_1 \\ \left[ \frac{\partial R_2}{\partial A(1)} \right]_1 & \left[ \frac{\partial R_2}{\partial A(2)} \right]_1 & - (R_2)_1 \end{vmatrix}
 \end{aligned}$$

39. Improved estimates  $(A(1))_2$ ,  $(A(2))_2$ , and  $(B)_2$  are found from:

$$(A(1))_2 = (A(1))_1 + \Delta A(1)$$

$$(A(2))_2 = (A(2))_1 + \Delta A(2)$$

$$(B)_2 = (B)_1 + \Delta B$$

these improved estimates are sufficiently accurate if  $(P_2)_2$ ,  $(G)_2$  and  $(R_2)_2$  are all sufficiently close to zero. If not, the process is repeated using  $(A(1))_2$ ,  $(A(2))_2$ ,  $(B)_2$  as the new guessed solutions. This procedure has been found to be consistently convergent in situations where solutions are possible. For evaluation of the terms containing partial derivatives, see Annex A.

DERIVATION OF INDIVIDUAL WHEEL LOADS

40. Figure 7 is developed by assuming that the plane PQRS is parallel to plane WXYZ (ground level), fixed to the vehicle chassis and contains a two dimensional coordinate system such that  $OO^1 = H_1$  with major axes parallel to those of the coordinate system in plane WXYZ. It is also assumed that each wheel of the vehicle is attached to the chassis via a suspension system which applies downward forces  $W_1(I)$  ( $I = 1$  to  $N$ ) at the  $I$ th wheel which is a function  $S$  of the vertical movement  $D_4(I)$  ( $I = 1$  to  $N$ ) of the wheels relative to the chassis from an unloaded position.

41. "Vertical" is defined as parallel to  $OO^1$ , and the chassis pitch and roll angles  $T_9$  and  $G_9$  are assumed to be sufficiently small, such that, errors in assuming that wheel deflections  $D_4(I)$  always take place in a vertical direction can be neglected.

42. The CG of the vehicle chassis is assumed to lie on plane PQRS when all suspension deflections are equal to  $K_1(K)$ .  $K_1(K)$  is a distance associated with each wheel pair or axle, and is defined as the vertically downward movement of an unloaded wheel resulting from adjustment of the suspension relative to the chassis, away from a position which places the wheel/ground contact point of the unloaded wheel in plane WXYZ when  $OO^1 = H_1$ .

43. Wheel loads were adjusted during the course of testing TV1000, as reported in Ref D, by adjusting the positions of suspension spring anchorages relative to the chassis. This effect was modelled by introducing  $K_1(K)$ . Values of  $K_1(K)$  for TV1000 were not given, but estimated values were found by trial and error, as described in Para 83. Normally, all  $K_1(K) = 0$ , i.e. the wheel/ground contact points of unloaded wheels lie in a single plane, normally parallel to a suitable reference plane on the chassis.

44. The coordinate system created in plane PQRS is considered to be fixed to the vehicle chassis. When forces  $W_3$ ,  $D_9$  and  $T$  are applied at the CG position, points in plane PQRS vertically above the wheel/ground contact points in plane WXYZ will adopt new positions in plane  $P'Q'R'S'$  as shown in Fig 3. The vertical movement of these points will be equal to the vertical movement of the wheel/ground contact points relative to the chassis,  $D_4(I)$ .

45. The suspension deflections are given by:

$$D_4(I) = D_0 + L(K) \sin(T_9) + C(J) \sin(G_9) + K_1(K) \quad - (3-1)$$

The height  $H$  of the CG above plane WXYZ is:

$$H = H_1 - (D_0 + L(N/2 + 1) \sin(T_9) + C(3) \sin(G_9)) \quad - (3-2)$$

where  $L(N/2 + 1)$  and  $C(3)$  are the coordinates of the CG in the system attached to the chassis. Generally,  $L(N/2 + 1)$  and  $C(3)$  are small and  $D_0$  does not vary greatly.  $H$  was treated as constant within the calculations described below.



46. Certain arrangements for driving the wheels can cause forces  $W_2(I)$  to be applied to the  $I$ th wheel, independently of the suspension forces  $W_1(I)$ . Both  $W_1(I)$  and  $W_2(I)$  are considered to act vertically downwards. If the vertically upward force acting at the  $I$ th is  $W(I)$  then (as shown in par. 58 to 71):

$$W(I) = W_1(I) + W_2(I) \quad - (4-6)$$

47. Paragraphs 58 to 71 contain the derivation of  $W_2(I)$  for radius arm suspension and drive arrangements typical of those proposed for wheeled skid steering vehicles, as well as the derivation of  $W_2(I)$  for tracked vehicles.

48. If the function  $S\{D_4(I)\}$  relating  $D_4(I)$  and  $W_1(I)$  is linear, considerations of vehicle equilibrium leads to  $N$  linear equations which can be solved by matrix methods to provide the wheel loads  $W(I)$  directly, for given values of  $W_2(I)$ . However this approach could not be used for non linear  $S$ , which is a probable feature of a suspension designed for fast off road movement.

49. The following method of calculating  $D_0$ ,  $T_9$  and  $G_9$  from considerations of vehicle equilibrium uses on Newtons iteration in the same way as the method used in para 11 to 15 to calculate ICR coordinates. The method ultimately depends on evaluation of the suspension force  $S\{D_4(I)\}$  and spring rate  $\frac{\partial S\{D_4(I)\}}{\partial D_4(I)}$  for

given values of deflection  $D_4(I)$  being possible. Some suspension characteristics may require the use of data fitting (curve fitting) techniques in order to achieve this in a convenient manner, and a method used is described in Annex B.

50. Referring to Fig 1, denoting the moments of all externally applied forces acting about XY, WZ and OC As  $M(1)$ ,  $M(2)$  and  $M_0$  respectively:

$$M(1) = \sum_{I=1}^{\frac{N}{2}} W(I) * (C(1) - C(2)) - T * H - W_3 * (C(3) - C(2)) \quad - (3-3)$$

$$M(2) = \sum_{I=N/2+1}^N W(I) * (C(2) - C(1)) - T * H + W_3 * (C(1) - C(3)) \quad - (3-4)$$

$$M_0 = \sum_{K=1}^{\frac{N}{2}} (W(K) + W(N/2 + K)) * L(K) + D_1 * H - W_3 * L(N + 1) \quad - (3-5)$$

51. In the case of (3-3) and (3-4), positive moments are considered to be anticlockwise viewing in the direction  $L_0$ .  $C(2)$  is normally negative. The effect of chassis pitch and roll angles on the projection of distances  $C(3)$  and  $L(N+1)$  onto plane  $WXIZ$  has been neglected.

52. It is required to find  $D_0$ ,  $T_9$  and  $G_9$  such that  $M(1)$ ,  $M(2)$  and  $M_0$  are each close to zero. Equation (19) can then be used to find the

suspension deflections  $D4(I)$  and hence the suspension forces  $W1(I)$ . The wheel loads are then calculated using (4-6).

53. Initial values  $(M(1))_1$ ,  $(M(2))_1$ ,  $(M\theta)_1$ , are computed using initial estimates of  $(D\theta)_1$ ,  $(G9)_1$ , and  $(T9)_1$  via equations (3-1), (4-6) and the functional relationship between  $W1(I)$  and  $D4(I)$ . The initial estimates are normally  $(G9)_1 = (T9)_1 = 0$  and  $(D\theta)_1$  set to the value of suspension deflection obtained for a suspension force of  $W3/N$ . Forces  $W2(I)$  will have been computed separately and are treated as known constants within this section. (See "Overall Method of Computation" para 75 to 77).

54. If  $\Delta D\theta$ ,  $\Delta T9$  and  $\Delta G9$  are approximate errors in  $(D\theta)_1$ ,  $(T9)_1$ ,  $(G9)_1$ , then:

$$(M(1))_1 + \Delta D\theta \left[ \frac{\partial M(1)}{\partial D\theta} \right]_1 + \Delta T9 \left[ \frac{\partial M(1)}{\partial T9} \right]_1 + \Delta G9 \left[ \frac{\partial M(1)}{\partial G9} \right]_1 = 0 \quad - (3-6)$$

$$(M(2))_1 + \Delta D\theta \left[ \frac{\partial M(2)}{\partial D\theta} \right]_1 + \Delta T9 \left[ \frac{\partial M(2)}{\partial T9} \right]_1 + \Delta G9 \left[ \frac{\partial M(2)}{\partial G9} \right]_1 = 0 \quad - (3-7)$$

$$(M\theta)_1 + \Delta D\theta \left[ \frac{\partial M\theta}{\partial D\theta} \right]_1 + \Delta T9 \left[ \frac{\partial M\theta}{\partial T9} \right]_1 + \Delta G9 \left[ \frac{\partial M\theta}{\partial G9} \right]_1 = 0 \quad - (3-8)$$

where 1 denotes evaluation of the relevant function at the point  $(D\theta)_1$ ,  $(T9)_1$ ,  $(G9)_1$ .

55. Provided that the terms containing partial derivatives can be evaluated, the approximate errors can be found by solving the three linear equations (3-6), (3-7), (3-8) by methods identical with those used in Part 1. For evaluation of the terms containing partial derivatives, see Annex C.

56. Improved estimates of  $D\theta$ ,  $T9$ , and  $G9$  are then obtained:

$$\begin{aligned} (D\theta)_2 &= (D\theta)_1 + \Delta D\theta \\ (T9)_2 &= (T9)_1 + \Delta T9 \\ (G9)_2 &= (G9)_1 + \Delta G9 \end{aligned}$$

this process is repeated until the values obtained for  $M(1)$ ,  $M(2)$ ,  $M\theta$  by substitution of the improved estimates of  $D\theta$ ,  $T9$ ,  $G9$  into equations (3-1), (3-3), (3-4), (3-5) are sufficiently close to zero.

57. The speed of the method depends on the accuracy of the initial estimates of  $D\theta$ ,  $T9$ ,  $G9$ . If significant forces  $T$  and  $D9$  are applied to the vehicle, the wheel loads are far from equal and the first estimates for  $D\theta$ ,  $T9$ ,  $G9$  on the basis given above are inaccurate. Under these conditions, the iterative process requires several passes to reach equilibrium.

# EFFECT OF SUSPENSION AND FINAL DRIVE ARRANGEMENTS ON

## WHEEL LOADS

### Wheeled Vehicle

58. Figure 8 shows a suspension arrangement typical of proposed and actual wheeled skid steered vehicles. A radius arm is attached to the vehicle at O and can rotate relative to the hull about O. Concentric with the radius arm attachment at O is an input drive shaft which is part of the radius arm and is connected to an output shaft at A by mechanisms internal to the radius arm such as gears or a chaindrive, normally such that the input and output shaft rotate in the same direction. The wheel can rotate about A relative to the radius arm and is driven by the output shaft.

59. Torque  $M_3$  is shown being applied to the radius arm (not the concentric drive shaft) at O by the suspension medium. This torque can be replaced by a downward load  $W(I)$  applied to the radius arm at A such that:

$$W(I) = M_3 / (R_9 \cos(T_8(I))) \quad - (4-1)$$

60. In practice a pure torque is applied to the radius arm at O only if the suspension medium is inboard of point of attachment to the hull. Outboard suspension components (Gas strut, coil spring, etc) could be attached to the radius arm anywhere between O and A. In all cases, a moment  $M_3$  about O is generated and the equivalent downward force  $W(I)$  at A can be obtained from (4-1). Generally (and within the calculations described in Para 40 to 57) suspension force/deflection characteristics are given in terms of the vertical force  $W(I)$  for a given vertical deflection at A of  $D_4(I)$ .

61. Torque  $T_{IN}$  is shown being applied to the input drive shaft by the vehicle driveline with torque  $-T_2(I)$  being applied to the output drive shaft at A. The forces  $W(I)$  (vertical load),  $F_1(I)$  (forward propulsive force) and  $R_6(I)$  (resistance to forward motion) are transmitted onto the end of the radius arm at A, via the wheel. The wheel has torque  $T_2(I)$  applied to it by the output shaft.

62. Deformation of the tyre in forward motion is considered to result in a forward movement  $x$  of the contact point as shown. It is proposed that  $x$  is dependent on the input torque  $T_2(I)$  as follows:

$x = x_0 + T_2(I)/K_4$  where  $K_4$  is constant, and  $x = x_0$  when  $T_2(I)$  and  $F_1(I)$  are zero. Hence from consideration of wheel equilibrium with  $T_2(I)$   $- F_1(I) = 0$ :

$$x_0 = - \frac{W_9 \cdot R_6(I)}{2 \cdot W(I)} \quad (\text{ie } x_0 \text{ is + ive for rearward } R_6(I))$$

equilibrium of the wheel with non zero values of  $T_2(I)$  and  $F_1(I)$  gives:

$$T_2(I) - W(I) * x - (F_1(I) + R_6(I)) * W_9/2 = 0 \quad - (4-2)$$

$$\text{or } T_2(I) - W(I) * (x_0 + T_2(I)/K_4) - (F_1(I) + R_6(I)) * W_9/2 = 0$$

substituting for  $x_0$ :

$$T_2(I) = F_1(I) * (W_9/(2 * (1 - W(I)/K_4))) \quad - (4-3)$$

a value for  $K_4$  was estimated from data published in Ref D for TV1000 when climbing slopes. The value used was  $K_4 = 65400$ . This results in a value of  $x$  equal to 0.157 feet for  $T_2(I) = 7000$  ft lb, and would apply to the tyres specific to TV1000 only. (See para 89 - TV1000 - Tyre Contact Point Movement, for this derivation of  $K_4$ .)

63. Consider equilibrium of the radius arm in Fig 8:

$$T_{IN} - T_2(I) - M_3 + W(I) * R_9 * \cos(T_8(I)) - (F_1(I) + R_6(I)) * (R_9 * \sin(T_8(I))) = 0$$

substituting for  $M_3$  and  $T_2(I)$  from (4-1) and (4-2):

$$\begin{aligned} W(I) - W_1(I) &= (F_1(I) + R_6(I)) * \tan(T_8(I)) \\ &+ F_1(I) * W_9 * (1-R_8)/(2 * (1-W(I)/K_4)) * R_9 * \cos(T_8(I)) \end{aligned} \quad - (4-4)$$

where  $R_8 = T_{IN}/T_2(I)$ , equal to the speed reduction ratio of the radius arm assuming 100% transmission efficiency.

64. It can be seen from (4-4) that for  $T_8(I) = 0$  and/or  $R_8 = 1$ , that  $W(I) = W_1(I)$ . If a positive difference that exists between  $W(I)$  and  $W_1(I)$  is considered to be a downward force  $W_2(I)$  acting at A, then:

$$W(I) = W_1(I) + W_2(I) \quad - (4-5)$$

$W_2(I)$  would therefore appear on the left hand side of equation (4-4).

65. "Leading" as opposed to "trailing" radius arms imply  $290^\circ < T_8(I) < 90^\circ$ , in which case  $W_2(I)$  will normally be negative, or in an upward direction. For a radius arm angle of  $(180 - T_8(I))$ , equation (4-4) provides an identical absolute value of  $W_2(I)$ , the sign being changed. A term  $Z(K)$  ( $K = 1$  to  $N/2$ ) is introduced in (4-4) which is set to -1 or +1 depending on whether the radius arm 'leads' or 'trails' (as in Fig 9). Radius arm angles are then always measured as the smallest angle from horizontal. (4-4) becomes:

$$\begin{aligned} W_2(I) &= Z(K) * ((F_1(I) + R_6(I)) * \tan(T_8(I)) \\ &+ F_1(I) * W_9 * (1-R_8)/(2 * (1-W(I)/K_4)) * R_9 * \cos(T_8(I))) \end{aligned} \quad - (4-6)$$

66. The radius arm angle  $T8(I)$  of the  $I$ th radius arm may be found from the suspension deflection  $D4(I)$ , which will have been found as a result of the determination of  $W(I)$ :

$$T8(I) = \sin^{-1} ((R9 * \sin(T7) - (D4(I) - D6 - K1(K)) / R9) \quad - (4-7)$$

where  $D6$  is defined as the suspension deflection which occurs when the radius arm angle is  $T7$ . Normally  $D6$  is set to the deflection appropriate to a suspension load of  $W3/N$ , and  $T7$  set to the suspension arm angle desired in the case of the vehicle standing still on level ground. The actual suspension arm angles  $T8(I)$  with the vehicle in a static condition will depend also on wheel spacings  $L(K)$ , suspension settings  $K1(K)$  and CG position  $L(N/2 + 1)$ ,  $C(3)$ .

#### Tracked Vehicle

67. The skid steering analysis developed in this document for wheeled vehicles can readily be applied to tracked vehicles, apart from the foregoing section dealing with effects of torque application at each wheel. A tracked vehicle with  $N$  road wheels is shown in Fig 9. The track/road wheel contact points can be defined by  $L, C$  coordinates as shown in Fig 2. The assumption that the whole of each wheel load is transferred onto the track/ground contact point immediately below each track/wheel contact point is consistent with the analysis being limited to vehicle behaviour on hard ground. Thus each track behaves as a longitudinally rigid body which is in contact with the ground at  $N/2$  points, and the theory set out in para 23 to 38 for determination of track/ground ICR is applicable. The wheel loads  $W(I)$  can be found by the method given in "derivation of Individual Wheel Loads" para 40 to 57. The manner of application of sliding forces at the track/ground contact points is considered to modify the forces  $W(I)$  by generation of forces  $W2$  as shown in Fig 8.

68. Each track has a force  $F3(J)$  applied at one end to cause sliding during skid steering. The track is assumed to be slack at the opposite 'end', immediately prior to passing below a road wheel. The track forces are given by:

$$F3(J) = \sum_{K=1}^{N/2} F1(I)$$

this is not equal to the total propulsive force  $F(J)$  developed by each 'track' as given by (2-6). As shown in Fig 9,  $F3(1)$  will normally be positive,  $F3(2)$  negative. In each case, a vertical force  $W2(I)$  is developed at the road wheel nearest the section of track under tension  $F3(J)$ . For consistency with (4-4) both  $W2(I)$  illustrated will be negative.

69. For positive  $F2$ :

$$W2((J-1) * N/2 + N/2) = -ABS(F3(J)) * \sin(L2) \quad - (4-8)$$

70. For negative F2:

$$W2((J-1) * N/2 + 1) = -ABS(F3(J)) * \sin(L1) \quad - (4-9)$$

all other W2 are assumed 0.

71. W2(I) as found by (4-8) and (4-9) for tracked vehicles frequently result in negative values of W(I) implying that the road wheel in question would be raised from the ground. (The calculation of W1(I) in (4-4) assumes that the track under the road wheel is in contact with the ground). In this instance W(I) must be set to zero, as well as  $\partial W1(I)/\partial D4(I)$  in equations (D-7), (D-8), (D-9) used to find chassis equilibrium. This requires suitable conditional statements in computer calculations. The reduction of wheel loads at the extremities of the vehicle in this way results in the remaining wheels carrying greater loads, but the overall effect is equivalent to shortening the wheelbase, which reduces opposition to slewing, and, generally, the values of A(J).

#### CALCULATION OF POWER INPUT AND DISSIPATION

##### Wheeled Vehicles

72. Referring to Fig 2, the N/2 contact points of a 'track' slide longitudinally (parallel to the vehicle centreline) and laterally (at right angles to the vehicle centreline) relative to the ground, at velocities V2(J) and -V2(J) \* Tan  $\theta(I)$  whilst generating forces F1(I) and P1(I) respectively. (Lateral velocity in the direction of the centre of turn is defined as negative.)

The total power dissipated in longitudinal and lateral sliding is therefore, for both 'tracks':

$$N4 = \sum_{I=1}^N F1(I) * V2(J) \quad - (5-1)$$

$$N5 = -\sum_{I=1}^N P1(I) * V2(J) * \tan \theta(I) \quad - (5-2)$$

the power input from the vehicle transmission to the wheels is given by:

$$N6 = (2/W9) * \sum_{I=1}^N T2(I) * V1(J) \quad - (5-3)$$

(V1(J) is the peripheral speed of the wheels relative to the hull or chassis and T2(I) is the torque input to each wheel.)

N6 normally exceeds (N4 + N5) due to power required to overcome motion resistance forces R6(I) and the additional torque required to drive the wheels due to contact patch movement.

73. T2(I) is usually negative for wheels on the 'inside' of the turn (I = N/2 + 1 to N) and this gives rise to negative power terms T2(I) \* V1(J) in (5-3), when V1(J) remains positive. This represents a power input to

the vehicle transmission by the wheel. The transmission would normally be designed to 'regenerate' this power at the wheels on the outside of the turn. The sum of wheel power inputs,  $N_6$  would equal engine power input to the transmission if the transmission efficiency including the efficiency of the regenerative path within it were 100%.

#### Tracked Vehicles

74. Equations (5-1) and (5-2) apply to the tracked vehicle steering on hard ground which has been considered within this report. The power input to the tracks cannot be found from (5-3), however and is given by:

$$N_6 = \sum_{J=1}^2 F_3(J) * V_1(J) \quad - (5-4)$$

or, alternatively

$$N_6 = \sum_{I=1}^N F_1(I) * V_1(J)$$

#### OVERALL METHOD OF COMPUTATION

75. This section describes the essential aspects of the logic of a computer program which utilises various sections and appendices of this document in order to calculate conditions applying to a skid steered vehicle in a turn of constant radius and speed.

76. Figure 10 does not include every logical step in the program, but shows the essential steps. For specified values of  $V$  and  $R$ , the longitudinal ICR coordinate  $B$  determines the magnitude of the inertia forces acting at the CG, however the method used to calculate  $A(J)$  and  $B$  requires these forces as input data. Hence an initial estimate of  $B$  is required, which is used to calculate initial values of the inertia forces and a resulting calculated value of  $B$ . An outer reiterative loop is used which provides new estimates of  $B$  based upon minimisation of the error (calculated  $B$  - estimated  $B$ ) using a linear iteration subroutine.

77. The calculation of wheel loads  $W(I)$  as detailed in Para 40 to 57 takes into consideration vertical forces  $W_2(I)$  which may be generated at each wheel, depending upon the specific driveline and suspension arrangements of the vehicle, and upon the torque applied to each wheel. Calculation of the wheel torques in turn depends on calculation of the ICR positions, which depends on  $W(I)$  as input data. Initial estimation of forces  $W_2(I)$  is difficult and so they are initially set to zero. Wheel loads  $W(I)$  and ICR coordinates are then calculated which result in new values of  $W_2(I)$ . These are used as new initial estimates, the process being repeated until stable values of  $W_2(I)$  are obtained. In practice this reiterative process converges fairly quickly.

PARTICULARS OF VEHICLES

78. The particulars of the vehicles are presented under the main headings TV1000, TV1333 and TV6000.

TV1000General

79. TV1000 was a 6 x 6 test vehicle built by the UK MOD Military Vehicles and Engineering Establishment (MVEE) in order to investigate the performance of a skid steered vehicle with large wheels. Reference D contains some data on the performance of TV1000 during skid steering. The following particulars, based on TV1000, were used as input data for computer calculations of skid steering performance, and were mostly taken from Ref D.

Leading Dimensions and Mass

- 80.
- |    |                                      |   |
|----|--------------------------------------|---|
| a. | Number of wheels (N):                | 6   |
| b. | Wheelbase :                          | 13.126 (Feet)   |
| c. | Track :                              | 8.876 (Feet)  |
| d. | Wheel Spacings: :                    | L(1) = 6.563, L(2) = 0,<br>L(3) = -6.563, C(1) = 4.438,<br>C(2) = -4.438 (Feet) |
| e. | CG Position :                        | H = 3.6, C(3) = 0,<br>L(4) = -0.21 (Feet)                                       |
| f. | Weight (W4) :                        | 46424 (lb)  |
| g. | Wheel Diameter<br>(effective) (D9) : | 4.72 (Feet)   |

Suspension Characteristics

81. The total wheel travel available on TV1000 is reported in Ref A to be adjustable in stages up to a maximum of 18 inches. The relationship between suspension force  $W_1(I)$  and wheel deflection  $D_4(I)$  was not given. It was assumed that the suspension geometry would have been designed to provide a 'rising' characteristic, with a maximum suspension force of magnitude  $2.5 \times W_4/N$  (19400 lb). The force/deflection relationship assumed is shown in Fig 11.

82. The proportion of vehicle mass carried on each wheel was measured during the course of testing TV1000 and the following average results reported in Ref D:

- |                |                              |
|----------------|------------------------------|
| Front wheels:  | 14224 lb (7112 lb per wheel) |
| Centre wheels: | 16464 lb (8232 lb per wheel) |
| Rear wheels:   | 15736 lb (7868 lb per wheel) |



83. The wheel loads calculated by the method given in para 40 to 57 assuming a static vehicle (ie, no skid steering or inertia forces being applied) were adjusted by varying the value of CG longitudinal coordinate  $L(4)$  and the centre suspension setting  $K1(2)$ . For  $L(4) = -0.21$  feet and  $K1(2) = 0.8$  inch, the following static wheel loads were calculated:

Front wheels:	14231 lb (7116 lb per wheel)
Centre wheels:	16477 lb (8238 lb per wheel)
Rear wheels:	15715 lb (7857 lb per wheel)

hence a value of  $-0.21$  ft was assumed for the CG coordinate  $L(4)$ , and the values assumed for  $K1(K)$  were  $K1(1) = 0$ ,  $K1(2) = 0.8$ ,  $K1(3) = 0$ .

#### Radius Arm Geometry

84. TV1000 was reported in Ref D to have 'leading' radius arms for the front wheels, and 'trailing' arms for the centre and rear wheels. In each case, the speed ratio  $R8$  of the driveline components within the radius arms was unity. Hence  $Z(1) = -1$ ,  $Z(2) = 1$ ,  $Z(3) = 1$ ,  $R8 = 1$ .

85. The length of the radius arms  $R9$  was assumed to be 3.0 feet.

86. It was necessary also to assume a value for the angle  $T7$ , the angle at which the radius arms would sit relative to a horizontal reference plane on the vehicle chassis, when each wheel is deflected by an amount equivalent to an applied load of  $W4/N$ . An angle of  $T7 = -8$  degrees (ie wheel hub centres nominally higher than the centres of rotation of the radius arms) was found to give the best match of calculated wheel torque figures. This is discussed in more detail below.

#### Friction Coefficients

87. Values for the lateral and longitudinal coefficients of friction between the wheels and the ground,  $M8$  and  $M9$ , had to be assumed. Values of 0.8 were suggested for  $M8$  and  $M9$  in Ref 1 and these were tried initially. It was found necessary to decrease the value of  $M8$  relative to  $M9$  in order to reasonably match the steering ratio required to achieve the first gear turn radius recorded for TV1000, and to match the wheel power inputs recorded for a neutral turn. The values finally used for the calculations were  $M8 = 0.75$ ,  $M9 = 0.85$ .

#### Rolling Resistance

88. Reference D reports an estimate of the rolling resistance of TV1000 of 1000 lb on level ground. This would lead to a value of  $1000/46424 = 0.0215$  for  $K2$  in equation (5), para 28. A value of 0.02 was used for  $K2$  in the calculations.

#### Tyre Contact Point Movement

89. Reference D contains the following data for TV1000 climbing directly up three slopes, with no application of steering brakes:

Slope (°)	Total Torque (LB-FT) To all Wheels
14	33107
18.4	39568
30	64972

90. To assess the extent of forward movement of the contact point of each wheel, it was assumed that each wheel provides equal propulsive force, with equal torque applied and equal movement of the contact point. In practice, the torques supplied to each wheel were not equal, particularly on the steepest slope. Equation (4-2) was then used to calculate a value of contact point movement  $x$  at each wheel for each slope value.

91. In this application of (4-2),  $(F1(I) + R6(I))$  was set to  $W4 * \sin(\text{Slope})/N$ ,  $W(I)$  to  $W4 * \cos(\text{Slope})/N$  and  $T2(I)$  to the torque value above, divided by  $N$ . This provides three values of  $x$  corresponding to the three slope values. These values, together with a value calculated for  $T2(I) = F1(I) = 0$  are shown in Fig 12. The broken line shown in Fig 12 passing close to the four data points was used to obtain a value of  $K4$  in equation (4-3) of 65400 lb.

### TV1333

#### General

92. TV1333 is the identification of a fictitious 8 x 8 wheeled skid steered vehicle which is intended to reflect TV1000 had it been built as an 8 x 8. It was assumed that an 8 x 8 vehicle designed for the same mission as a 6 x 6 would weigh more due to the possible increase in total hull length imposed by the combination of the additional running gear, and the likely need to minimise any reduction in wheel diameter so that ground pressure is not increased.

#### Leading Dimensions and Mass

93. a. Number of wheels (N): 8
- b. Weight : 51066 lb  
(A 10% weight increase was assumed)

94. The wheel spacings were obtained by first considering the wheel diameter. In order to keep nominal ground pressure the same as TV1000, the area of each tyre in contact with the ground per unit weight carried was made equal to TV1000. It was assumed that the contact area is proportional to diameter x section width of tyre, and that the diameter/section width ratio is not changed. Hence for a 10% total mass increase, the ratio of wheel diameters for TV1000/TV1333 is given by  $\sqrt{1.1}$  x  $6'$ , which leads to an effective wheel diameter of 4.285 feet for TV1333. The longitudinal spaces between the wheels were reduced from 1.6 feet for TV1000 to 1.0 feet for TV1333. (This results in a hull length increase of approximately 6% for TV1333, compared with TV1000). The resulting wheel

spacings were:  $L(1) = 7.927$ ,  $L(2) = 2.642$ ,  $L(3) = -2.642$ ,  $L(4) = -7.927$ ,  
 $C(1) = 4.488$ ,  $C(2) = -4.488$  (Feet).

95. The small increase in track compared with TV1000 is due to the decrease in section width of the tyres used for TV1333. It was assumed that the overall width of the vehicle would remain the same as TV1000. Thus:

- c. Wheelbase : 15.854 (Feet)
- d. Track : 8.976 (Feet)
- e. CG Position :  $H = 3.6$ ,  $C(3) = 0$ ,  
 $L( ) = -0.25$  (Feet)

#### Suspension Characteristics

96. The 18 inch total wheel travel of TV1000 was retained, the same general shape of suspension force/wheel travel curve retained, the force being scaled down by a factor  $1.1 \times 6/8$ . All  $K1(K)$  were set = 0.

#### Radius Arm Geometry

97. All radius arms were made 'trailing', since it seemed likely that economy in length of driveline paths offered by front leading arms on the 6 x 6 might not be as advantageous with an 8 x 8, and that possible production cost economies resulting from a common radius arm and suspension layout might be attractive. Thus all  $Z(K) = 1$ . Radius arm length  $R9$  was assumed to be 2.7 feet. The nominal angle  $T7$  corresponding to radius arm position for a wheel deflection equivalent to an applied load of  $W4/N$  was set to  $0^\circ$ , ie the vehicle would be intended to stand on level ground in a static condition with all radius arms in a horizontal position, assuming that all wheel loads were equal.

#### Friction Coefficients

98. The values chosen for TV1000 were used, ie  $M8 = 0.75$ ,  $M9 = 0.85$ .

#### Rolling Resistance

99. The value used for TV1000 was adopted, ie,  $K2 = 0.02$ .

#### Tyre Contact Point Movement

100. The value of  $K4$  used was increased to reflect the small tyre size of TV1333, and consequent smaller contact point movement which might be expected to occur,  $K4 = 73000$ .

### TV6000

#### General

101. TV6000 is the identification used for a hypothetical tracked vehicle which is intended to reflect TV1000 had it been built as a tracked vehicle, with twelve road wheels.

### Leading Dimensions and Mass

- 102.
- |    |                                       |   |   |
|----|---------------------------------------|---|---|
| a. | Number of road wheels (N)             | : | 12  |
| b. | Wheelbase (road wheels)               | : | 13.126 (Feet)   |
| c. | Track                                 | : | 8.876 (Feet)  |
| d. | Road wheel spacings                   | : | L(1) = 6.563, L(2) = 3.937;<br>L(3) = 1.312, L(4) = -1.312,<br>L(5) = -3.937, L(6) = -6.563,<br>C(1) = 4.438, C(2) = -4.438<br>(Feet) |
| e. | CG Position                           | : | H = 3.6, C(3) = 0,<br>L(7) = -0.2 (Feet)  |
| f. | Weight                                | : | 46424 (lb)  |
| g. | Road Wheel Diameter                   | : | Not used in calculations for<br>tracked vehicle.  |
| h. | Track approach and<br>departure angle | : | 30 degrees  |

### Suspension Characteristics

103. The 18 inch wheel travel of TV1000 was retained, and suspension force, increasing linearly to a maximum of approx 2.5\* W4/N (9700 lb) was assumed, as shown in Fig 13. It was found that some combinations of forces acting on the vehicle could cause individual wheels to reach full deflection, and it was necessary to model a 'bump stop'. This was done by adding an additional inch to the wheel travel in which the suspension force rises steeply from 9700 to 30000 lb. All K1(K) were set = 0.

### Radius Arm Geometry

104. As detailed in para 40 to 57, the determination of wheel loads W(I) for a tracked vehicle for the calculations described in this report depends upon the track tension F3(J) and the track approach and departure angle L1 and L2, rather than the radius arm geometry and torque applied to each wheel, the latter being zero for a tracked vehicle. The calculation of radius arm position angles T8(I) was retained for reference, for this purpose the nominal setting angle T7 was made 0 and the radius arm length R9 set to 2 feet.

### Friction Coefficients

105. Values of  $M8 = M9 = 0.8$  were used, which are assumed to be consistent with the track being equipped with rubber pads for operation on hard surfaces.

## Rolling Resistance

106. The rolling resistance of a tracked vehicle would be expected to be greater than for a wheeled vehicle. Ref D used a factor of 0.04 for obtained total rolling resistance of a tracked vehicle from total weight.

This was in effect adopted for the calculations within this report, ie  $K2 = 0.04$ . The method of application of  $K2$  (via equation (5) in para 28) results in the rolling resistance generated by each track being unequal if unequal proportions of vehicle weight are carried by each track. Hence the total rolling resistance of the vehicle will always be  $W3 * K2$ , with an additional moment applied to the vehicle if the rolling resistance of the tracks are unequal, resisting turning if the more heavily loaded track is on the outside of the turn.

107. Tyre Contact Point Movement - not applicable.

#### RESULTS OF SKID STEERING CALCULATIONS

##### TV1000 - Torque Input to Individual Wheels

108. Equation (4-3) gives the relationship assumed between forward propulsive force  $F1(I)$  at an individual wheel and torque input  $T2(I)$ . For a given ICR position,  $F1(I)$  is dependant in turn on the vertical load  $W(I)$  and  $\theta(I)$  as assumed in equation (2-1). Equations (4-5) and (4-6) summarise the relationship assumed between wheel load  $W(I)$  and torque input  $T2(I)$ , radius arm position angle  $T8(I)$ , radius arm reduction ratio  $R8$ , radius arm length  $R9$ , tractive force ( $F1(I) + R6(I)$ ). For given positive tractive force and torque input, the wheel load  $W(I)$  is increased if  $T8(I) > 0$  and/or  $R8 < 1$ . Increase in wheel load will, through the iterative process described in para 77, cause the torque input calculated for that particular wheel to be increased.

109. For TV1000,  $R8 = 1$  and the measured wheel input torques shown in Table 1, are consistently lower in magnitude for centre wheels providing positive propulsive force (wheel No 2) compared with centre wheels providing negative propulsive force (wheel No 5). This pattern could only be reproduced in the calculations by making  $T8(I) < 0$ . The calculated figures in Table 1 were obtained for  $T7 = -8^\circ$  which made  $T8(I) < 0$ . This would imply that the normal position of the wheel centres are higher from the ground than the centres of rotation of the radius arms, an unexpected situation. At the time of writing this document, there was no other information available on the nominal radius arm position for TV1000. Acquisition of such additional data would provide a useful test for the theoretical assumptions made here.

110. It can be seen quickly from Table 1 that the theory gives good estimates for wheel torque input only at lower radius of turn. For fourth gear, the calculated values of wheel input torques are up to 175% greater in magnitude than the measured torques. This level of error is not, however, reflected in the calculated value of steering ratio and total wheel power input, which remain in reasonably close agreement with the measured values. The error in torque levels is considered likely to be an effect of tyre lateral flexibility, which was not considered in this analysis.

TABLE 1 - MEASURED AND CALCULATED WHEEL INPUT TORQUES FOR TV1000  
(FIGURES IN PARENTHESES INDICATE INPUT DATA FOR CALCULATIONS)

	Total Speed Ft/S	Radius of Turn Feet	Wheel Speed V1, Ft/3		Steering Ratio	Power Input To Whts	TORQUE INPUT (LB-FT) TO INDIVIDUAL WHEELS						Remarks
			Inner	Outer			1	2	3	4	5	6	
Measured			-3.01	2.62	-0.87	148.2	8540	15470	9830	-7360	-18120	-9290	'Neutral' Gear
Calculated	(-0.237)	(-0.94)	-2.90	2.54	-0.874	152.1	10500	15101	10578	-8058	-17248	-11077	
Measured		20.54	1.01	3.34	3.064	67.25	10910	17400	10630	-9780	-18660	-10000	1st Gear
Calculated	(2.15)	(20.5)	1.125	3.33	2.964	62.8	10925	15210	10807	-8039	-18113	-10922	
Measured		46.58	6.73	10.11	1.502	107.0	10740	14400	10410	-9410	-14770	-8360	2nd Gear
Calculated	(8.42)	(46.5)	6.517	10.35	1.583	111.2	11281	15634	10258	-8640	-17384	-10853	
Measured		73.5	11.85	15.21	1.284	115.1	10540	10160	12260	-9170	-11780	-8640	3rd Gear
Calculated	(13.53)	(73.5)	11.483	15.41	1.342	118.1	11588	15851	9776	-9024	-16779	-10802	
Measured		115.6	19.6	22.95	1.171	119.5	7608	7406	5244	-5070	-5715	-4800	4th Gear
Calculated	(21.44)	(115.6)	19.18	23.23	1.211	131.7	12158	15933	8975	-9442	-15822	-10715	

#### Variation of Steering Ratio, Power Input and Power Dissipation with Radius of Turn

111. Figure 14 shows calculated values of steering ratio  $S$  ( $S$  is defined in para 20, equation (1-6)) for TV1000 travelling at negligible forward speed on flat ground, for a range of radii of turn,  $R$ .  $S$  increases steadily with reduction of  $R$  from large positive values, and approaches infinity as  $V_1(2)$  approaches zero, or the 'inside' track become stationary with respect to the vehicle hull. Negative values of  $S$  start to occur as  $V_1(2)$  becomes negative, or the 'inside' track moves forward relative to the hull. For  $S = -1$  (tracks moving in opposite directions at equal speeds relative to the hull) the radius of turn is close to zero.  $S = 0$  occurs when the 'outside' track speed  $V_1(1)$  becomes zero and the radius of turn is about -10 ft.

112. Figure 15 shows the calculated effect of total speed on the relationship between  $S$  and  $R$  within a range of practical turn radii, for TV1000. for  $V = 20$  and 30 ft/sec, a lower limit to radius of turn was found to affect the calculation procedure as programmed for computer solution. Below these limiting radii, solution to the equilibrium equations (2-10 to 2-12) was not found. The total inertia (centrifugal) force applied to the vehicle at these radii are equivalent to 0.73 and 0.78 respectively of vehicle mass. Given the friction coefficients assumed between wheels and ground, it could reasonably be expected that a limit to vehicle equilibrium would occur close to these turn radii. As the vehicle approaches the limiting turn radii at the higher speeds, the change in steering ratio for change in turn radius becomes zero, and in the case of  $V = 30$ , becomes negative before the limiting turn radius is reached. This suggests a regime of negative steering stability, ie that a reduction in steering ratio could cause a decrease rather than an increase in turn radius.

113. The calculated power input to the wheels for steady turns under such conditions, however, is very high and suggests that the lower limit to turn radius at a given speed would in practice be higher than those suggested by Fig 15. Fig 16 shows the total power dissipated in sliding of wheel contact points ( $N_4 + N_5$ ) and the total power input to the wheels ( $N_6$ ) plotted against radius of turn  $R$  for a total speed  $V$  of 20 ft/sec, for TV1000. Practical considerations of engine power for a vehicle this size could be expected to impose a lower limit of about 40 feet radius for a steady turn at this speed.

114. Figures 17 and 18 show the calculated relationship between steering ratio  $S$  and radius of turn  $R$  for TV1333 and TV6000 (tracked). The general shape of the relationships for various forward speeds are not significantly different to those calculated for TV1000, and the limiting turn radii at the various higher speeds are nearly the same. The hypothetical tracked vehicle TV6000 requires a generally lower level of steering ratio for a given radius of turn. This is reflected in the lower values of  $A(J)$  found for the tracked vehicle, compared with the wheeled vehicles under equivalent conditions, and is consistent with the prediction in Ref 2 of a decrease in turning radius for an increase in number of wheels, for a given steering ratio and wheelbase/track ( $L/C$ ) ratio. The values of  $A(J)$  calculated for TV1333 were not significantly less than for TV1000 because the  $L/C$  ratio of TV1333 was increased, to accommodate eight wheels with ground pressure equivalent to TV1000.

115. The power dissipated in sliding of wheel/ground contact points ( $N_4 + N_5$ ), is dependant on the slip velocities  $V_2(J)$  as given by equations (5-1) and (5-2).  $V_2(J)$  are in turn proportional to  $A(J)$  as given by equation (1-9) and hence it could be expected that power dissipation of "equivalent" vehicles could be related to comparative levels of  $A(J)$ . Figures 16, 19, 20 show relationships between calculated power dissipated in wheel/track sliding ( $N_4 + N_5$ ), calculated power input to wheels/tracks  $N_6$  (see equations (5-3) and (5-4)) for various values of turn radius  $R$ , for a total vehicle speed of 20 ft/sec. The calculated power dissipation in sliding for the tracked vehicle TV6000TR is significantly less than for the two wheeled vehicles. The power dissipation in sliding for TV1333 exceeds that for TV1000 due to the greater weight assumed for the 8 x 8 vehicle, and slightly greater levels of  $A(J)$ . In all cases the power input  $N_6$  exceeds the power dissipation. This is due mainly to the work required to overcome motion resistance as defined by equation (2-5), and in the case of the wheeled vehicles, additional work done when the wheel input torques are increased by tyre contact point movement, as defined by equation (4-3). The latter assumption was applied to the wheeled vehicles only, and is the reason for the difference (power input - power dissipated in sliding) being greater in their case than for the tracked vehicle.

#### Steering on Slopes

116. Skid steering calculations were performed for the three vehicles operating on a sloping plane as shown in Fig 21. Negligible forward speed  $V$  was assumed, making the inertia force terms (equations 1-4 and 1-5) zero, longitudinal and lateral forces at the vehicle CG resulting from components of the vehicle weight only (equations 1-10, 1-11 and 1-12).

117. Figure 19 shows a set of results obtained for TV1000 for a slope angle ( $T_3$ ) of  $38^\circ$ , for various heading angles ( $G_8$ ). For  $G_8$  below  $4$

degrees and greater than 43 degrees, the procedures for finding A(J) and B were not convergent. The physical interpretation of this is that the vehicle is unable to generate skid steering forces which are in equilibrium with the externally applied forces when attempting a steady turn outside of these heading angle limitations. The heading angle limitations therefore define part of an 'envelope' within which the vehicle is able to steer by skid steering, in accordance with all the assumptions made. Fig 22 shows that for  $G8 = 22$  degrees, A(2) makes a transition from negative to positive values. This implies that the slip velocity V2(2) of the wheels on the inside of the turn makes a transition from negative to positive values (see equation 1-9), and for  $G8 = 22$  to  $G8 = 43$ , both rows of wheels will have positive slip velocity, and hence generate positive propulsive forces.

118. By re-casting equation (1-6), it is possible to calculate R2 and hence R, for given S.

$$(R = \text{SQR} (R2 + 2 + (B * L(1) - C(3)) + 2))$$

for a steering ratio S of 3 (a typical 'first gear' value), calculated R increased from 12.4 feet to 98.8 feet as  $G8$  increased from 4 to 43 degrees, indicating that a significant reduction in rate of turn can be expected to be associated with turns carried out at the higher limit of heading angle  $G8$ , for a slope angle of 38 degrees.

119. Figure 20 summarizes the envelope within which solutions to the skid steering calculations were found to be possible for TV1000, for heading angles between 0 (parallel to slope) and 90 (straight up slope). The envelope indicates that at high values of T3 and  $G8$ , both rows of wheels or 'tracks' must develop positive slip velocities, or positive propulsive forces, which is consistent with overcoming the high longitudinal force which results from operation at high values of T3 and  $G8$ . A suitable physical explanation for the overall shape of the envelope has not been sought. It is considered likely that the large 'no-go' or 'no-steer' area between  $G8 = 55$  and  $G8 = 90$  results from the coulomb friction assumption of equations (2-1) and (2-2), which fix the level of the forces developed by sliding of the wheels, irrespective of the speed of sliding. For  $G8 = 90$ , the greatest possible slope angle was found to be  $T3 = 13.5$  degrees. At this point, the 'inner' 'track' was in negative slip, or generating negative propulsive force. The 'outer' 'track' was developing positive propulsive force to overcome that of the 'inner' 'track', together with the longitudinal component of vehicle weight implied by equation 1-12. This accounts for the smaller maximum slope for  $G8 = 90$  than for  $G8 = 0$ .

120. Figures 22 and 23 show the envelope of skid steering solutions, or 'slope steerability diagrams' calculated for TV1333 and TV6000TR. The envelope shape for TV1333 is essentially similar to that of TV1000, except that the 'no-steer' area at high heading angles is marginally smaller, and the greatest possible slope for both  $G8 = 0$  and  $G8 = 90$  is higher. The envelope shape for TV6000TR is significantly different at high values of  $G8$  to those of TV1333 and TV1000. For  $G8 = 90$ , the greatest possible slope angle with the inside track generating negative propulsive force was  $T3 = 14$ . Solutions were also found for  $G8 = 90$  with the 'inside' track generating positive propulsive force at  $T3 = 27$  and  $T3 = 28$  indicating that the tracked vehicle might be expected to operate without limit on slopes of these angles. Calculation of the envelope, however, indicated a small 'no-go' area centred on  $G8 = 48$ ,  $T3 = 28$  which could theoretically impede



operation over a small range of heading angles. The significance of the small 'no-steer' area, which appears in a similar position on the diagrams for TV1000 and TV1333, has not been investigated further.

121. The ability of the tracked vehicle to operate at significantly higher slope angles when facing straight up the slope, compared with the wheeled vehicles, is attributed to the vehicle suspension characteristics and the interaction of the propulsive forces with the running gear.

122. The tracked vehicle is mounted on a relatively large number of road wheels, each of which is attached to a suspension which under static conditions is required to provide a force of (vehicle mass normal to ground)/(number of road wheels) or  $(W_3/N)$ . For large  $N$ , suspension forces are modest compared with vehicle mass. This results in relatively low pitch stiffness, when compared with a vehicle of similar proportions supported by fewer wheels. When facing up a steep slope, the vehicle will 'sit back' on the rearmost road wheels and tend to lift the front wheels clear of the ground. If both tracks are generating positive propulsive forces, the associated track tension will tend to raise the rear road wheels, or reduce the load they carry. This will enhance the nose-up tendency and further concentrate the support of vehicle weight on fewer road wheels. This effectively 'shortens' the vehicle without affecting its width between tracks, or effectively reduces its L/C ratio. This results in the vehicle being 'easier' to turn in that the moment generated by the tracks when slowing, which must be overcome by the moment generated by the difference in track propulsive forces, is reduced.

123. Table 2 shows the wheel loads  $W(I)$  calculated for the three vehicles considered at the extreme 'top right hand corner' of their slope steerability envelopes. The wheeled vehicles show considerable transfer of load onto the rear wheels from the front wheels, but not a significant reduction in the proportion of the total load carried at the extremities (front and rear) of the vehicles. The wheel loads calculated for the tracked vehicle, however, show the concentration of load onto the central road wheels which can be expected to improve the ability of the vehicle to turn under these conditions.

TABLE 2 - WHEEL LOADS CALCULATED FOR TV1000, TV1333 AND TV6000TR  
AT EXTREMES OF SLOPE ANGLE (T3) HEADING ANGLE (G8) ENVELOPES

TV1000					TV1333					TV600TR				
	CA	A(1)	A(2)	B	T3	CA	A(1)	A(2)	B	T3	CA	A(1)	A(2)	B
	83			44.3	36	83			55.7	28	90	13.01	0.12	-0.50
WHEEL N (1)	LOAD W(I) (1b)	WHEEL (1)	LOAD W(I) (1b)	WHEEL (1)	LOAD W(I) (1b)	WHEEL (1)	LOAD W(I) (1b)	WHEEL (1)	LOAD W(I) (1b)	WHEEL (1)	LOAD W(I) (1b)	WHEEL (1)	LOAD W(I) (1b)	
	2473.9	4	1529.0	1	2182.2	5	1375.6	1	221.6	7	0.0			
	7177.6	5	6346.4	2	4478.0	6	3763.0	2	2031.6	8	1142.6			
	10499.0	6	9562.8	3	6620.8	7	5944.5	3	3862.5	9	2973.4			
				4	8844.4	8	8104.8	4	5692.7	10	4803.6			
								5	7523.5	11	6634.5			
								6	1163.8	12	4940.2			

TRACK TENSIONS:  
OUTER  $[F_3(1)] = 16382.9$  (1b)  
INNER  $[F_3(2)] = 7051.4$  (1b)

CONCLUSIONS

124. In common with the predictions of Ref A and Ref B the results of the numerical calculations indicate that wheeled vehicles require a significantly higher level of steering ratio or "track speed difference" to achieve a given radius of turn than an "equivalent" tracked vehicle. This results in a higher power requirement, generally, for skid steering of wheeled vehicles than tracked vehicles.

125. The relationship between steering ratio and radius of turn predicted for each vehicle under conditions of steady turning at high speeds suggest unstable steering characteristics, but this occurs under conditions where the predicted power requirements exceed the likely power output of the vehicle power plants. Given the assumptions of the numerical calculations, therefore which include relatively high values of friction coefficient for ground/vehicle frictional forces, each vehicle would be expected to steer in a stable fashion when performing steady (constant speed and radius) turns.

126. The range of slope angles and slope heading angles over which the numerical calculations predict that skid steering is possible was similar for the two wheeled vehicles considered. The limiting slope angle for heading straight up the slope was significantly lower than for heading parallel with the slope. This, and the general shape of the envelope of slope and heading angles calculated, suggests that the ability of the wheeled vehicles to steer up slopes might be significantly reduced when the heading angle exceeds 50-55 degrees. This agrees with practical experience reported in Ref D and other documents, in relation to TV1000, but it must be remembered that the practical results were obtained with the vehicle on soft ground.

127. For the tracked vehicle, the limiting slope angle for heading straight up the slope was significantly higher than for the wheeled vehicles. The envelope of slope and heading angle calculated for the tracked vehicle included a discontinuity at slope angles below the limiting slope angle. This is attributed to the nature of the vehicle/ground friction assumption, which requires frictional forces to be developed irrespective of the speed of the tracks over the ground. It is concluded that the tracked vehicle can be expected to steer over a wider range of slope and slope heading angles than the wheeled vehicles. The higher limiting slope angle when heading straight up the slope for the tracked vehicle is attributed to the inherent ability of the suspension and running gear to modify the road wheel load distribution in a way which favours skid steering.

128. Experimental data, including wheel torque inputs, exist for TV1000 performing turns on hard ground at fairly low speeds (Ref D). The results of the numerical calculations performed for TV1000 under equivalent conditions are in good agreement with the measurements at small radii of turn, but at larger radii, the calculated wheel torque input levels are too high. This is attributed to lack of suitable consideration of tyre flexibility within the numerical calculations.

### RECOMMENDATIONS

129. Using the method of analysis developed in this document, it would be possible to obtain an indication of the effects of various changes in vehicle design upon the steering performance of wheeled and tracked skid steered vehicles on smooth hard ground. Under certain conditions, the method of analysis is subject to errors, but the results obtained can be used as comparative rather than absolute indications of steering performance. Should such additional information be required, the following features are recommended for investigation of their potential for improvement of skid steering performance of wheeled vehicles:

- a. Radius arms (attaching wheels to chassis) which enclose driveline components with an output/input speed ratio of less than 1.
- b. Irregular longitudinal spacing of wheel pairs, and variation in the proportion of vehicle weight carried by each wheel, the latter being introduced by deliberate variation of the force/deflection relationship of each wheel suspension.
- c. Variation of the vehicle CG position.

130. The method developed for analysis of skid steering performance of wheeled vehicles on smooth hard ground does not adequately allow for the effects of tyre flexibility, and this leads to inaccurate results at large turn radii. Inclusion of tyre flexibility effects in the hard ground skid steering performance analysis is likely to be of less interest to Users than preparation of a soft ground skid steering analysis. Analysis of skid steering of wheeled vehicles on soft ground is considered unlikely to require inclusion of tyre flexibility effects, but would need to be accompanied by a tracked vehicle soft ground skid steering analysis, in order to compare wheeled and tracked vehicles.

131. If further development of skid steering analysis is desirable, the following topics are recommended for consideration, in the order of priority shown:

- a. Wheeled vehicle skid steering on soft ground.
- b. Tracked vehicle skid steering on soft ground.
- c. Inclusion of tyre flexibility effects in the analysis of wheeled vehicle skid steering on ground.

132. Each of these topics could be expected to require significantly more resources to implement them than was required to complete the work reported in this document. Expenditure of such effort should be preceded by a survey of similar work which other agencies may be undertaking.

#### List of Annexes:

- A. Evaluation of Partial Derivative Terms Required to Define Estimates of ICR Coordinates
- B. Use of Data Fitting Procedure for Calculation of Suspension Forces and Suspension Spring Rates

- C. Evaluation of Partial Derivative Terms required to Refire  
Estimates of Vehicle Hull Altitude
- D. Illustrations

EVALUATION OF PARTIAL DERIVATIVE TERMS REQUIRED TO REFINESTIMATES OF ICR COORDINATES

1. By inspection of equations (2-10), (2-11), (2-12):

$$\frac{\partial P_2}{\partial A(1)} = \frac{\partial M(1)}{\partial A(1)} - C(1) * \frac{\partial F(1)}{\partial A(1)} \quad - (A1)$$

$$\frac{\partial P_2}{\partial A(2)} = \frac{\partial M(2)}{\partial A(2)} - C(2) * \frac{\partial F(2)}{\partial A(2)} \quad - (A2)$$

$$\frac{\partial P_2}{\partial B} = \frac{\partial M(1)}{\partial B} + \frac{\partial M(2)}{\partial B} - C(1) * \frac{\partial F(1)}{\partial B} - C(2) * \frac{\partial F(2)}{\partial B} \quad - (A3)$$

$$\frac{\partial G_2}{\partial A(1)} = \frac{\partial F(1)}{\partial A(1)} \quad - (A4)$$

$$\frac{\partial G_2}{\partial A(2)} = \frac{\partial F(2)}{\partial A(2)} \quad - (A5)$$

$$\frac{\partial G_2}{\partial B} = \frac{\partial F(1)}{\partial B} + \frac{\partial F(2)}{\partial B} \quad - (A6)$$

$$\frac{\partial R_2}{\partial A(1)} = \frac{\partial P(1)}{\partial A(1)} \quad - (A7)$$

$$\frac{\partial R_2}{\partial A(2)} = \frac{\partial P(2)}{\partial A(2)} \quad - (A8)$$

$$\frac{\partial R_2}{\partial B} = \frac{\partial P(1)}{\partial B} + \frac{\partial P(2)}{\partial B} \quad - (A9)$$

2. In order to evaluate the right hand sides of equations A1 thru A9, expressions are required for:

$$\frac{\partial M(J)}{\partial A(J)}, \frac{\partial F(J)}{\partial A(J)}, \frac{\partial P(J)}{\partial A(J)}, \frac{\partial M(J)}{\partial B}, \frac{\partial F(J)}{\partial B}, \frac{\partial P(J)}{\partial B} \quad (J = 1, 2)$$

From (8):

$$\frac{\partial M(J)}{\partial A(J)} = M_9 \sum_{K=1}^{\frac{N}{2}} L(K) * W(I) * \frac{\partial}{\partial A(J)} (\sin \theta(I)) \quad - (A10)$$

From (6):

$$\frac{\partial F(J)}{\partial A(J)} = M8 \sum_{K=1}^{\frac{N}{2}} W(I) * \frac{\partial}{\partial A(J)} (\cos \theta(I)) \quad - (A11)$$

From (7):

$$\frac{\partial P(J)}{\partial A(J)} = -M9 \sum_{K=1}^{\frac{N}{2}} W(I) * \frac{\partial}{\partial A(J)} (\sin \theta(I)) \quad - (A12)$$

From (8):

$$\frac{\partial M(J)}{\partial B} = M9 \sum_{K=1}^{\frac{N}{2}} L(K) * W(I) * \frac{\partial}{\partial B} (\sin \theta(I)) \quad - (A13)$$

From (6):

$$\frac{\partial F(J)}{\partial B} = M8 \sum_{K=1}^{\frac{N}{2}} W(I) * \frac{\partial}{\partial B} (\cos \theta(I)) \quad - (A14)$$

From (7):

$$\frac{\partial P(J)}{\partial B} = -M9 \sum_{K=1}^{\frac{N}{2}} W(I) * \frac{\partial}{\partial B} (\sin \theta(I)) \quad - (A15)$$

These equations are derived by supposing that of the terms included in (2-6), (2-7), (2-8) only  $\sin \theta(I)$  and  $\cos \theta(I)$  ( $I = 1, N$ ) are functions of  $A(1)$ ,  $A(2)$  and  $B$ .

3. Expressions for  $\frac{\partial}{\partial A(J)} (\sin \theta(I))$ ,  $\frac{\partial}{\partial A(J)} (\cos \theta(I))$ ,  $\frac{\partial}{\partial B} (\sin \theta(I))$

and  $\frac{\partial}{\partial B} (\cos \theta(I))$  may be found by differentiating (2-3) and (2-4):

$$\frac{\partial}{\partial A(J)} (\sin \theta(I)) = -A(J) * (L(1))^2 * (L(K) - B * L(1)) * ((L(K) - B * L(1))^2 + (A(J) * L(1))^2)^{-3/2} \quad - (A16)$$

$$\frac{\partial}{\partial A(J)} (\cos \theta(I)) = L(1) * ((L(K) - B * L(1))^2 + (A(J) * L(1))^2)^{-1/2} \\ - (A(J))^2 * (L(1))^3 * ((L(K) - B * L(1))^2 + (A(J) * L(1))^2)^{-3/2} \quad - (A17)$$

$$\frac{\partial}{\partial B} (\sin \theta(I)) = L(1) * (L(K) - B * L(1))^2 * ((L(K) - B * L(1))^2 + (A(J) * L(1))^2)^{-3/2} \\ - L(1) * ((L(K) - B * L(1))^2 + (A(J) * L(1))^2)^{-1/2} \quad - (A18)$$

$$\frac{\partial}{\partial B} (\cos \theta(I)) = -A(J) * (L(1))^2 * (L(K) - B * L(1)) * ((L(K) - B * L(1))^2 + (A(J) * L(1))^2)^{-3/2} \quad - (A19)$$

Note that  $\frac{\partial}{\partial B} (\cos \theta(I)) = -\frac{\partial}{\partial A(J)} (\sin \theta(I))$

USE OF DATA FITTING PROCEDURE FOR CALCULATION OF SUSPENSIONFORCES AND SUSPENSION SPRING RATES

1. If the force/deflection characteristic of a suspension can be accurately represented by a series of straight lines, little problem should be experienced in writing a subroutine for a computer program which gives suspension force  $W1(I)$  and suspension rate  $\frac{\partial W1(I)}{\partial D4(I)}$  for given  $D4(I)$ .

2. This procedure may also be acceptable where the straight lines are a reasonable approximation to the smooth curve that some suspensions may exhibit. If greater accuracy is desired, a curve can be fitted to data selected from the suspension characteristic.

3. A 'cubic spline' data fitting routine supplied with volume 2 of the Maths Manual "Plot 50", supplied in support of the Tektronix 4054 computer was used for calculation of suspension forces generated by non linear suspensions.  $(N1 + 1)$  pairs of data points  $(W1(M), D5(M))$ ,  $M = 1$  to  $(N1 + 1)$  are used to generate a  $N1 \times 4$  array of coefficients  $C3(J, K)$  ( $J = 1$  to  $N1$ ,  $K = 1$  to 4). Then for  $D5(J) \leq D4(I) \leq D5(J + 1)$ .

$$W1(I) = C3(J,1) + C3(J,2) * (D4(I) - D5(J)) + C3(J,3) * (D4(I) - D5(J))^2 + C3(J,4) * (D4(I) - D5(J))^3$$

$$\frac{\partial W1(I)}{\partial D4(I)} = C3(J,2) + 2 * C3(J,3) * (D4(I) - D5(J)) + 3 * C3(J,4) * (D4(I) - D5(J))^2 \quad (I = 1 \text{ to } N)$$



EVALUATION OF PARTIAL DERIVATIVE TERMSREQUIRED TO REFINE ESTIMATES OF VEHICLE HULL ATTITUDE

1. It has been shown in part 4 that  $W(I) = W_1(I) + W_2(I)$  ( $I = 1$  to  $N$ ) and stated that during computation of  $W(I)$  by the method given in section 3,  $W_2(I)$  remain constant. Hence from equations (3-3), (3-4), (3-5)

$$\frac{\partial M(J)}{\partial D\theta} = (2J - 3) * \sum_{K=1}^{\frac{N}{2}} \frac{\partial W_1(I)}{\partial D\theta} * (C(1) - C(2)) \quad - (C-1)$$

$$\frac{\partial M(J)}{\partial D\theta} = \sum_{K=1}^{\frac{N}{2}} \left[ \frac{\partial W_1(K)}{\partial D\theta} + \frac{\partial W_1}{\partial D\theta} (N/2 + K) \right] * L(K) \quad - (C-2)$$

$$\frac{\partial M(J)}{\partial T\theta} = (2J - 3) * \sum_{K=1}^{\frac{N}{2}} \frac{\partial W_1(I)}{\partial T\theta} * (C(1) - C(2)) \quad - (C-3)$$

$$\frac{\partial M\theta}{\partial T\theta} = \sum_{K=1}^{\frac{N}{2}} \left[ \frac{\partial W_1(K)}{\partial T\theta} + \frac{\partial W_1}{\partial T\theta} (N/2 + K) \right] * L(K) \quad - (C-4)$$

$$\frac{\partial M(J)}{\partial G\theta} = (2J - 3) * \sum_{K=1}^{\frac{N}{2}} \frac{\partial W_1(I)}{\partial G\theta} * (C(1) - C(2)) \quad - (C-5)$$

$$\frac{\partial M\theta}{\partial G\theta} = \sum_{K=1}^{\frac{N}{2}} \left[ \frac{\partial W_1(K)}{\partial G\theta} + \frac{\partial W_1}{\partial G\theta} (N/2 + K) \right] * L(K) \quad - (C-6)$$

2. Using equation (3-1) to evaluate  $\frac{\partial D^4(I)}{\partial D\theta}$ ,  $\frac{\partial D^4(I)}{\partial T\theta}$ ,  $\frac{\partial D^4(I)}{\partial G\theta}$ :

$$\begin{aligned} \frac{\partial W_1(I)}{\partial D\theta} &= \frac{\partial W_1(I)}{\partial D^4(I)} * \frac{\partial D^4(I)}{\partial D\theta} \\ &= \frac{\partial W_1(I)}{\partial D^4(I)} \\ &= \frac{\partial (S \{D^4(I)\})}{\partial D^4(I)} \quad - (C-7) \end{aligned}$$

$$\begin{aligned}\frac{W_1(I)}{\partial T_9} &= \frac{\partial W_1(I)}{\partial D_4(I)} * \frac{\partial D_4(I)}{\partial T_9} \\ &= \frac{\partial (S \{D_4(I)\})}{\partial D_4(I)} * L(K) * \cos(T_9) \quad - (C-8)\end{aligned}$$

$$\begin{aligned}\frac{\partial W_1(I)}{\partial G_9} &= \frac{\partial W_1(I)}{\partial D_4(I)} * \frac{\partial D_4(I)}{\partial G_9} \\ &= \frac{\partial (S \{D_4(I)\})}{\partial D_4(I)} * C(J) * \cos(G_9) \quad - (C-9)\end{aligned}$$

3. Substituting (C-7) thru (C-9) in (C-1) thru (C-6):

$$\frac{\partial M(J)}{\partial D_0} = (2J - 3) * \sum_{K=1}^{\frac{N}{2}} \frac{\partial (S \{D_4(I)\})}{\partial D_4(I)} * (C(1) - C(2)) \quad - (C-10)$$

$$\frac{\partial M_0}{\partial D_0} = \sum_{K=1}^{\frac{N}{2}} \left[ \frac{\partial (S \{D_4(K)\})}{\partial D_4(K)} + \frac{\partial (S \{D_4(N/2 + K)\})}{\partial D_4(N/2 + K)} \right] * L(K) \quad - (C-11)$$

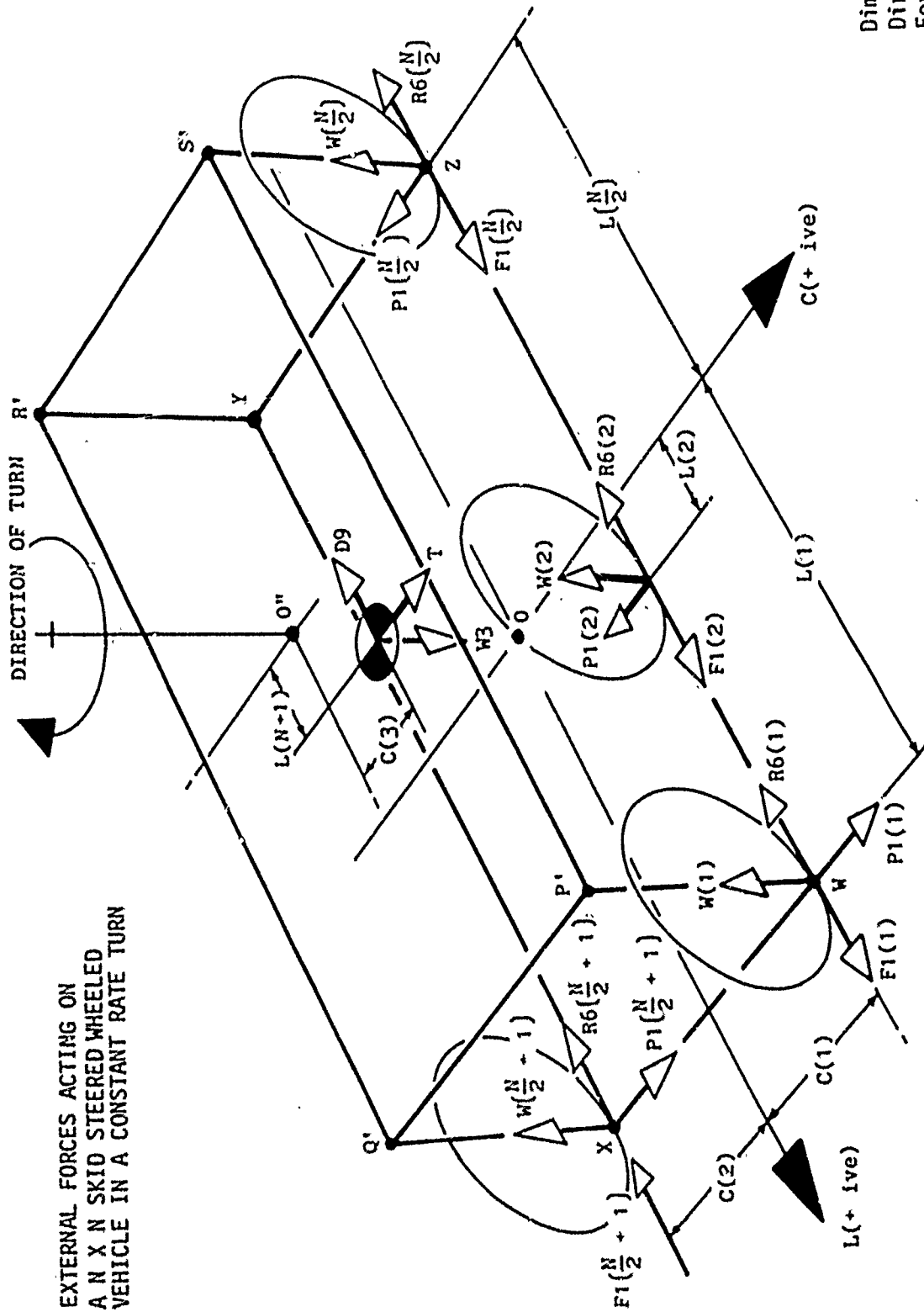
$$\frac{\partial M(J)}{\partial T_9} = (2J - 3) * \sum_{K=1}^{\frac{N}{2}} \frac{\partial (S \{D_4(I)\})}{\partial D_4(I)} * (C(1) - C(2)) * L(K) * \cos(T_9) \quad - (C-12)$$

$$\frac{\partial M_0}{\partial T_9} = \sum_{K=1}^{\frac{N}{2}} \left[ \frac{\partial (S \{D_4(K)\})}{\partial D_4(K)} + \frac{\partial (S \{D_4(N/2 + K)\})}{\partial D_4(N/2 + K)} \right] * L(K)^2 * \cos(T_9) \quad - (C-13)$$

$$\frac{\partial M(J)}{\partial G_9} = (2J - 3) * \sum_{K=1}^{\frac{N}{2}} \frac{\partial (S \{D_4(I)\})}{\partial D_4(I)} * (C(1) - C(2)) * L(K) * \cos(G_9) \quad - (C-14)$$

$$\frac{\partial M_0}{\partial G_9} = \sum_{K=1}^{\frac{N}{2}} \left[ \frac{\partial (S \{D_4(K)\})}{\partial D_4(K)} + \frac{\partial (S \{D_4(N/2 + K)\})}{\partial D_4(N/2 + K)} \right] * L(K) * C(J) * \cos(G_9) \quad - (C-15)$$

Equations (C-10) thru (C-15) provide values for all partial derivative terms contained in equations (3-6), (3-7), (3-8).



Dimension  $\rightarrow$   
 Direction  $\rightarrow$   
 Force  $\rightarrow$

FIG 1 - EXTERNAL FORCES ACTING ON  
A  $N \times N$  SKID STEERED WHEELED  
VEHICLE IN A CONSTANT RATE TURN

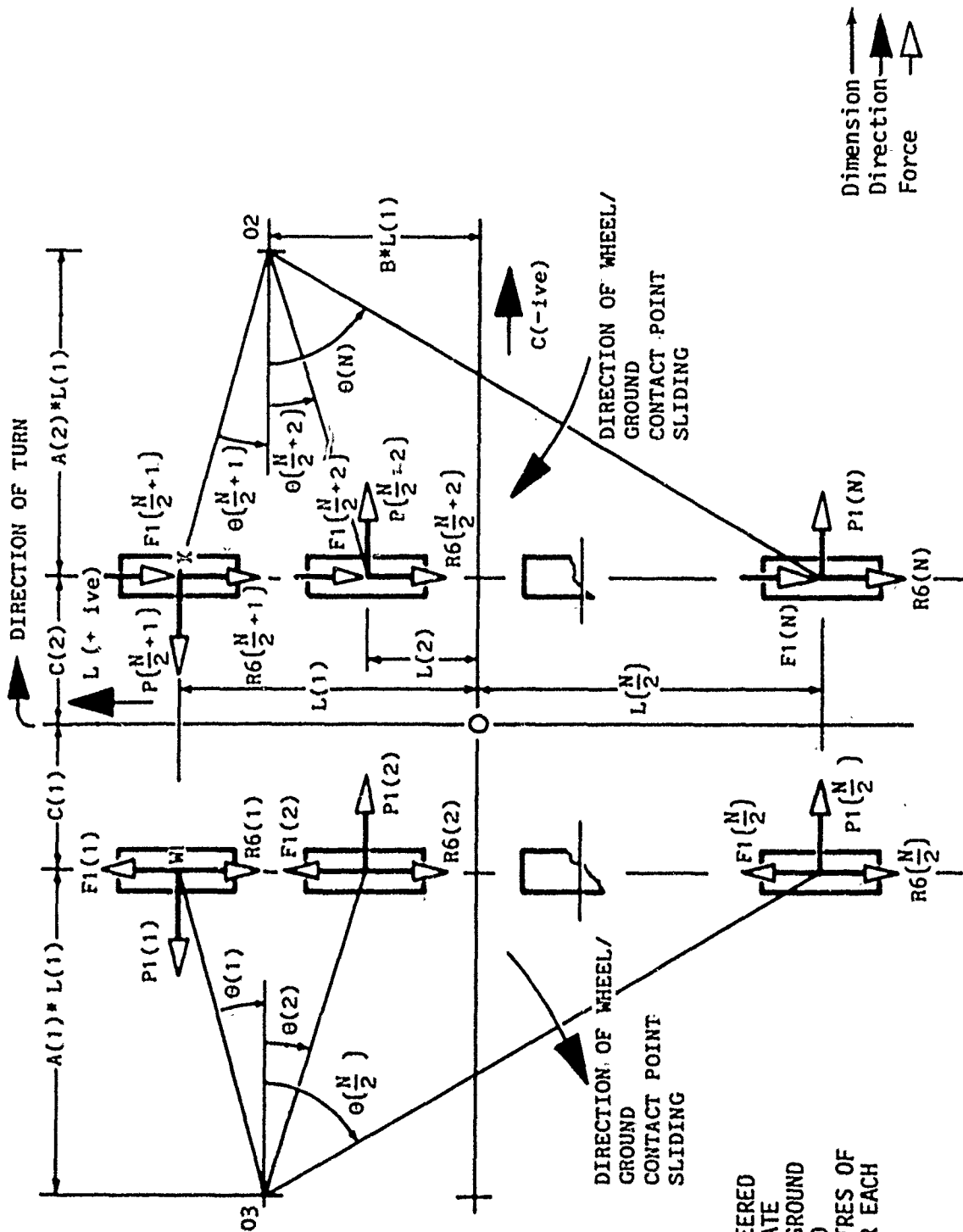
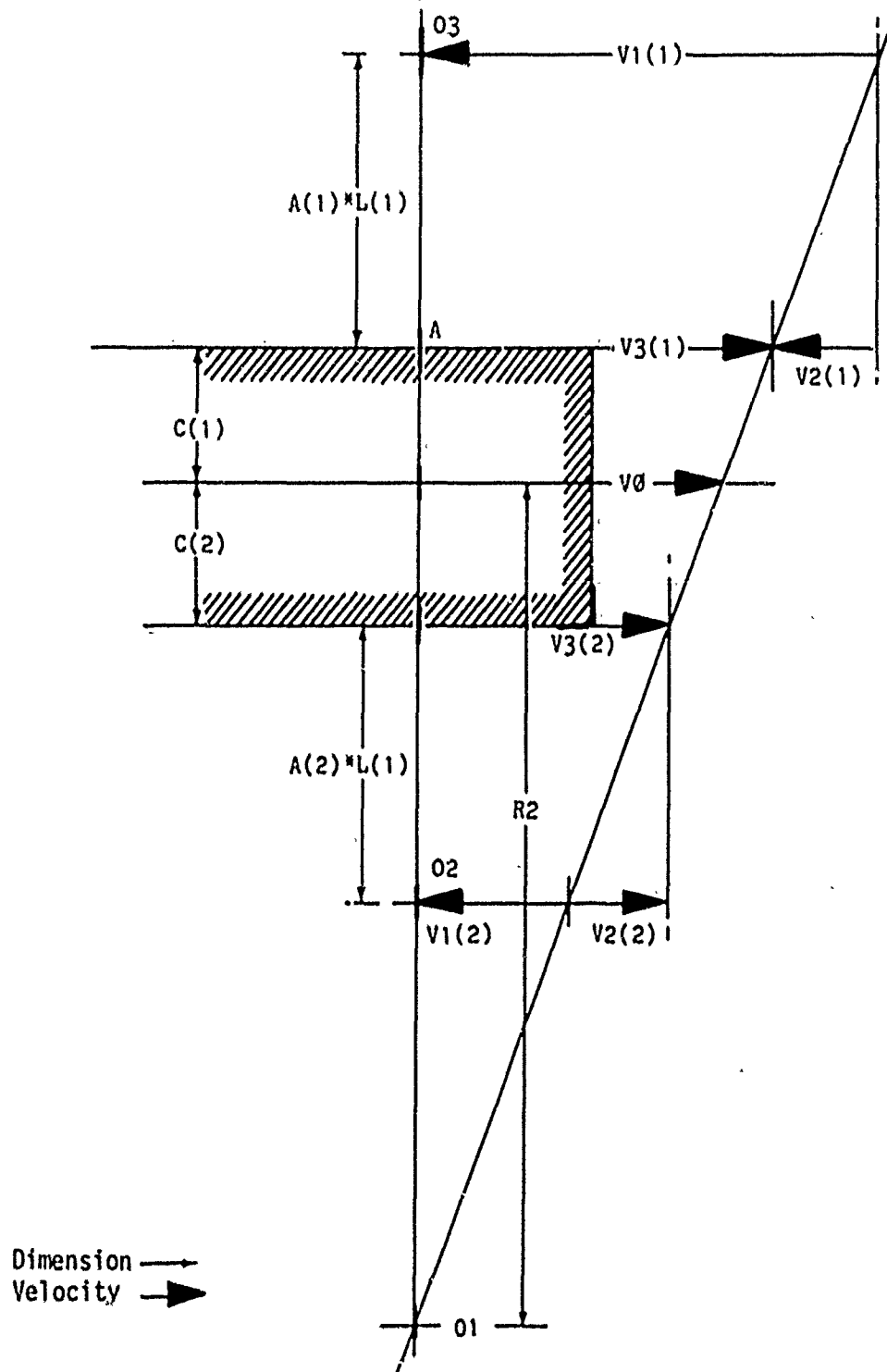


FIG 2 - N WHEELED SKID STEERED  
VEHICLE - COORDINATE  
SYSTEM FOR WHEEL/GROUND  
CONTACT POINTS AND  
(INSTANTANEOUS CENTRES OF  
ROTATION) (ICR) FOR EACH  
ROW OF WHEELS

Dimension  $\uparrow$   
Direction  $\blacktriangle$   
Force  $\triangle$

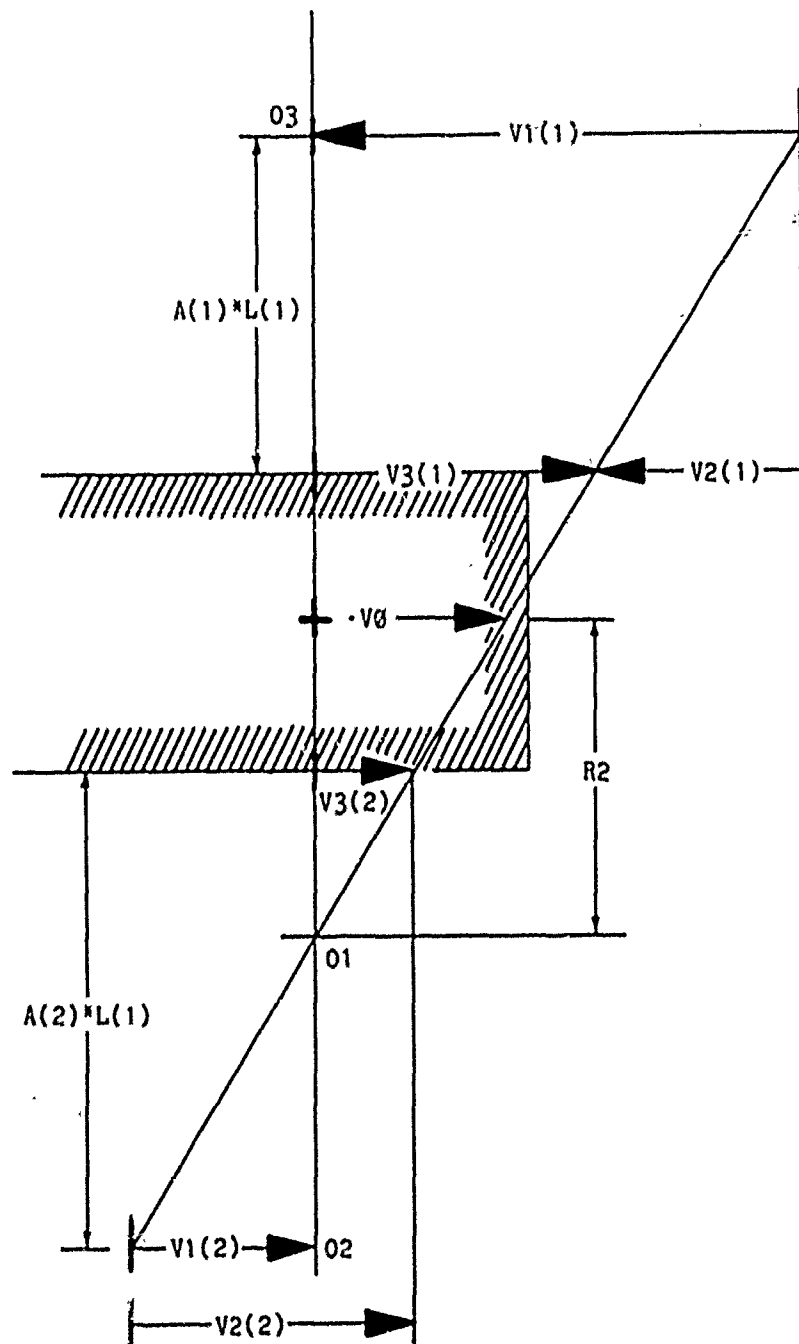


FIG 4 - VELOCITIES OF TRACKS RELATIVE TO HULL AND GROUND  
(Inner Track Moving Rearwards Relative to Hull)



- Notes: For  $J = 1$  (Outer),  $2$  (Inner), All Velocities are Resolved Parallel to Vehicle Centre Line
- $V0$  = Velocity of Hull at Centre Line
  - $V1(J)$  = Velocity of Tracks Relative to Hull
  - $V2(J)$  = Velocity of Tracks Relative to Ground (Slip Velocity)
  - $V3(J)$  = Velocity of Hull at Track Attachment Points

FIG 5 . VELOCITIES OF TRACKS RELATIVE TO HULL AND GROUND  
(Inner Track Moving Forwards Relative to Hull)



Dimension  $\rightarrow$   
Velocity  $\rightarrow$



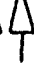
 Dimension  
 Direction  
 Force

FIG 6 - OPERATION OF VEHICLE ON SLOPE - RESOLUTION OF WEIGHT

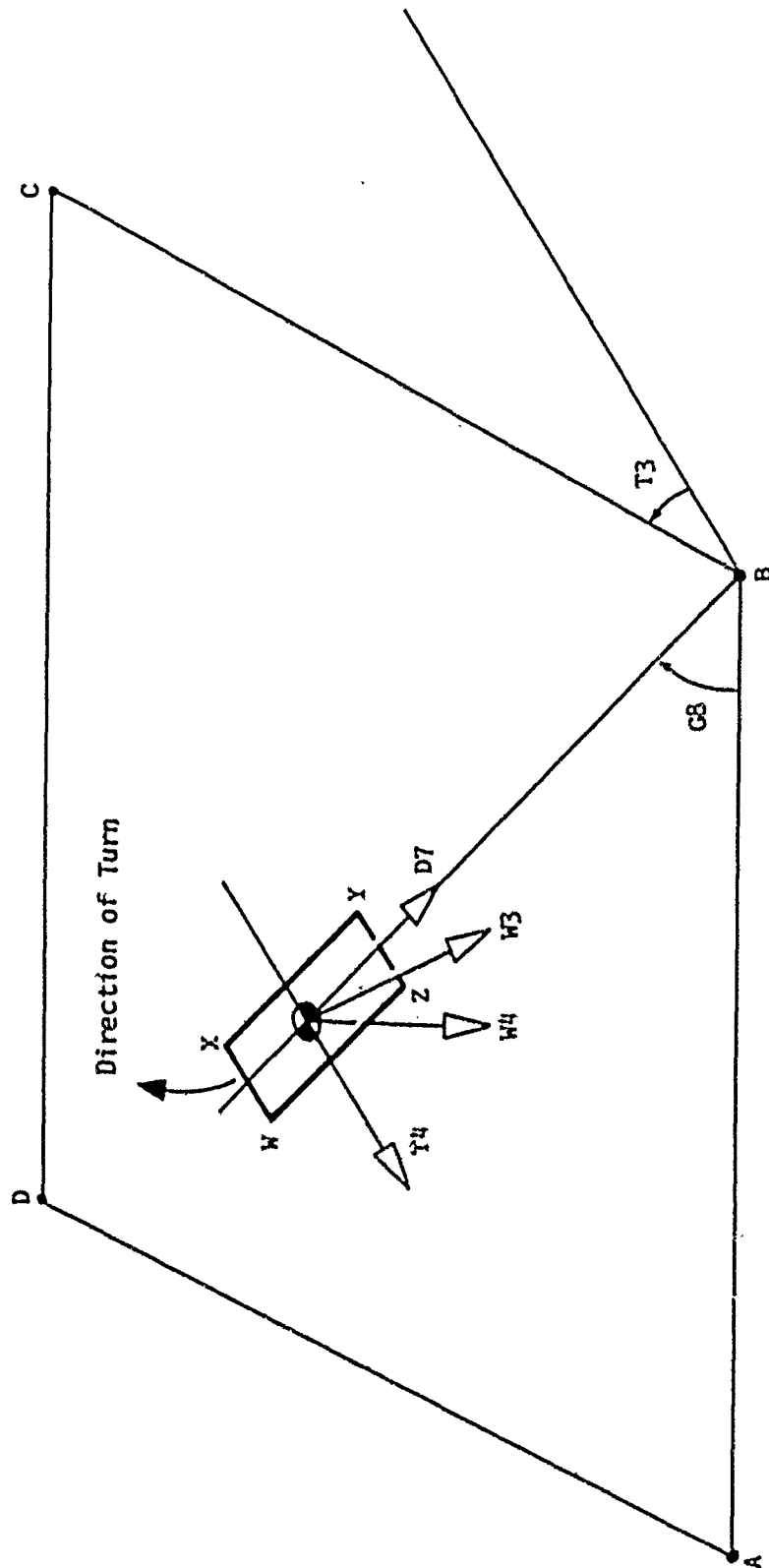
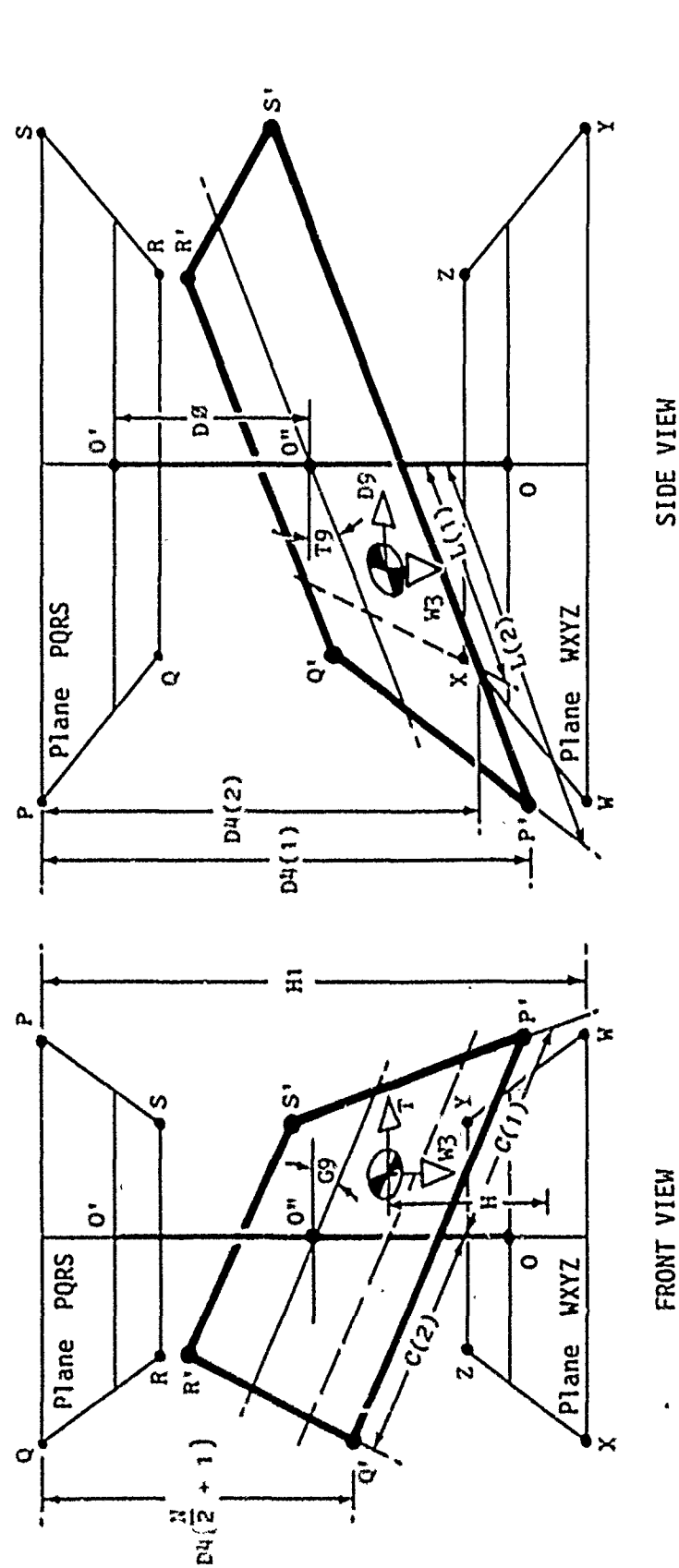




FIG 7 - SUSPENSION DEFLECTIONS AND CHASSIS ATTITUDE RESULTING FROM FORCES ACTING AT VEHICLE CofG (Unsprung Weight Assumed Zero)



Note: Chassis Roll Angle  $G9$  and Pitch Angle  $T9$  are Positive as Shown. Of Forces Acting on Chassis, Only Those Acting Through CofG are Shown.

FIG 8 - FORCES AND TORQUES ACTING ON INDIVIDUAL WHEELS AND SUSPENSION RADIUS ARMS (Wheeled Vehicle)(Drive to Wheel Transmitted Through Radius Arm)

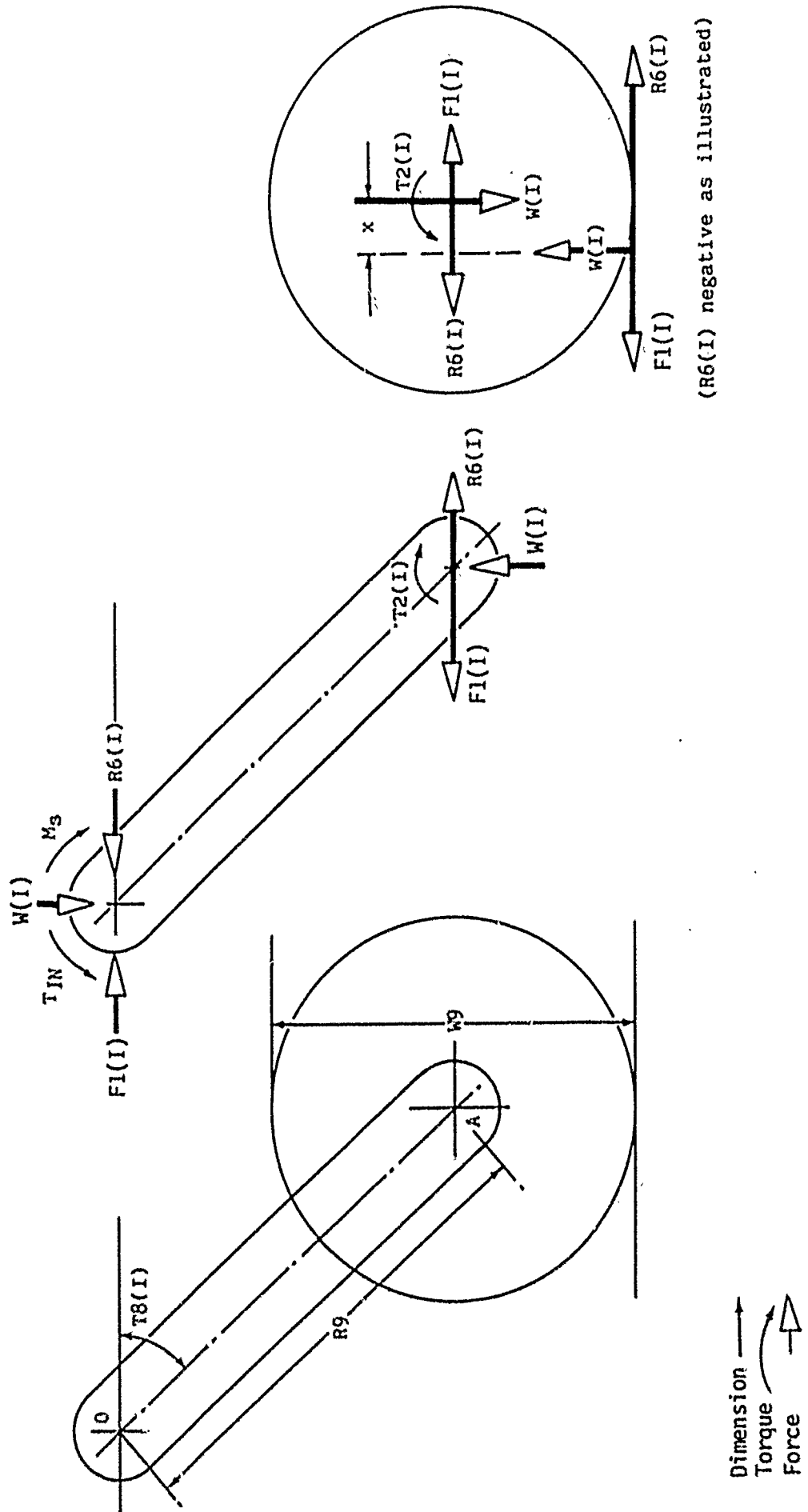


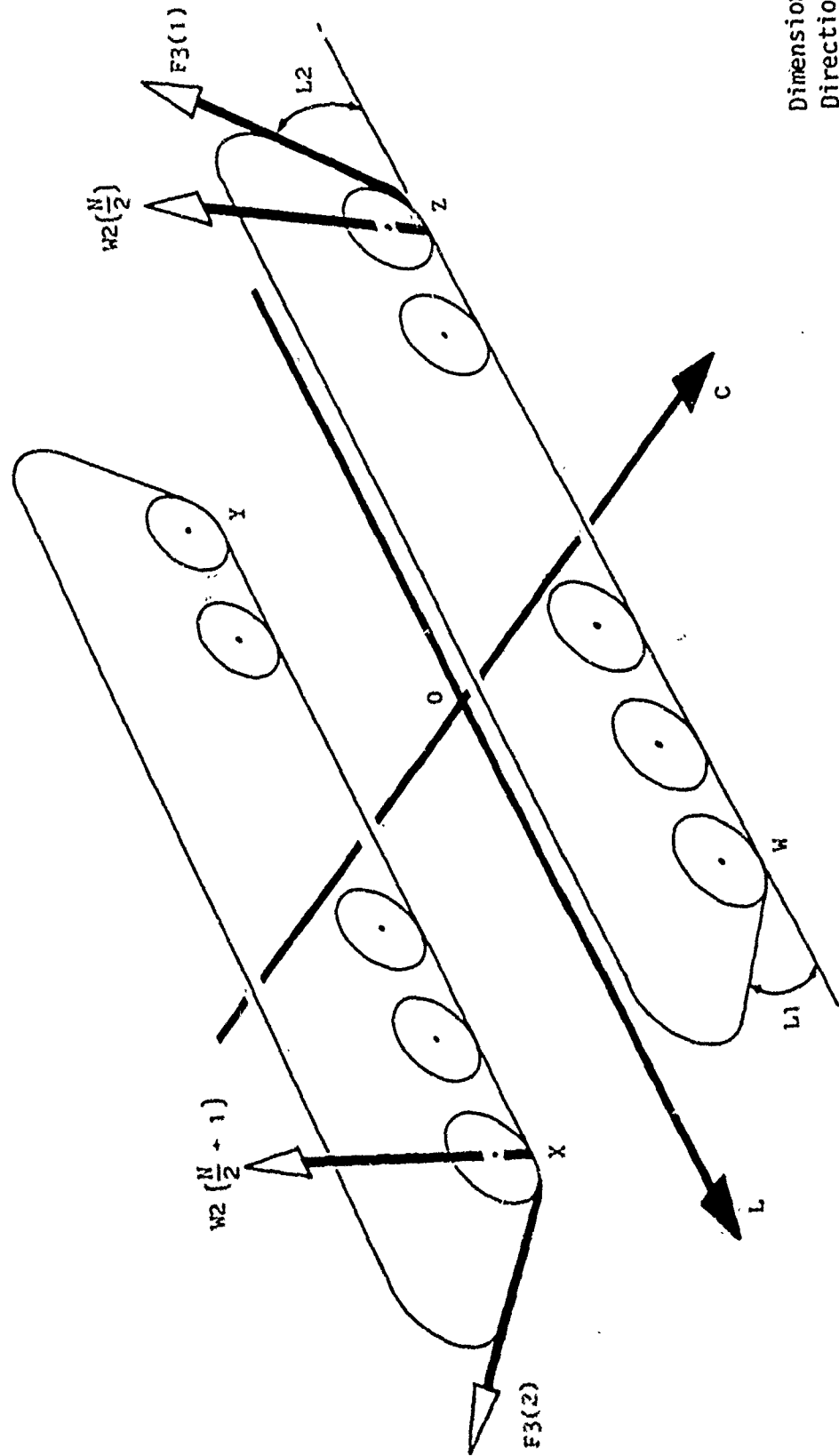
FIG 9 - TRACKED VEHICLE - TRACK FORCES  $F3(J)$  AND RESULTING FORCES AT WHEELSTracked Vehicle - Track Forces  $F3(J)$  and Resulting Wheel Loads  $W2$

FIG 10 - OVERALL METHOD OF COMPUTATION

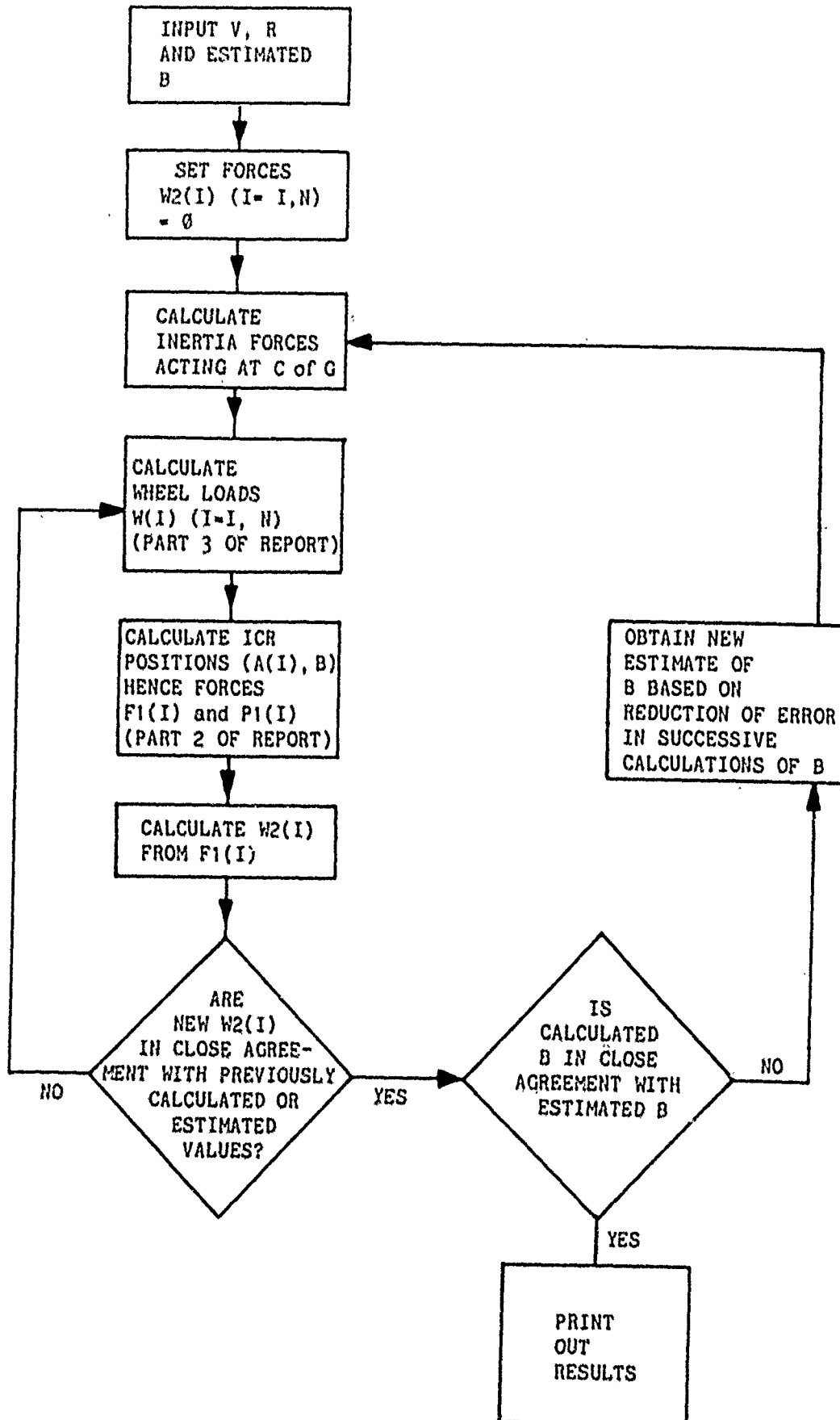


FIG 11 - TV1000 - ASSUMED SUSPENSION FORCE/DEFLECTION CHARACTERISTIC

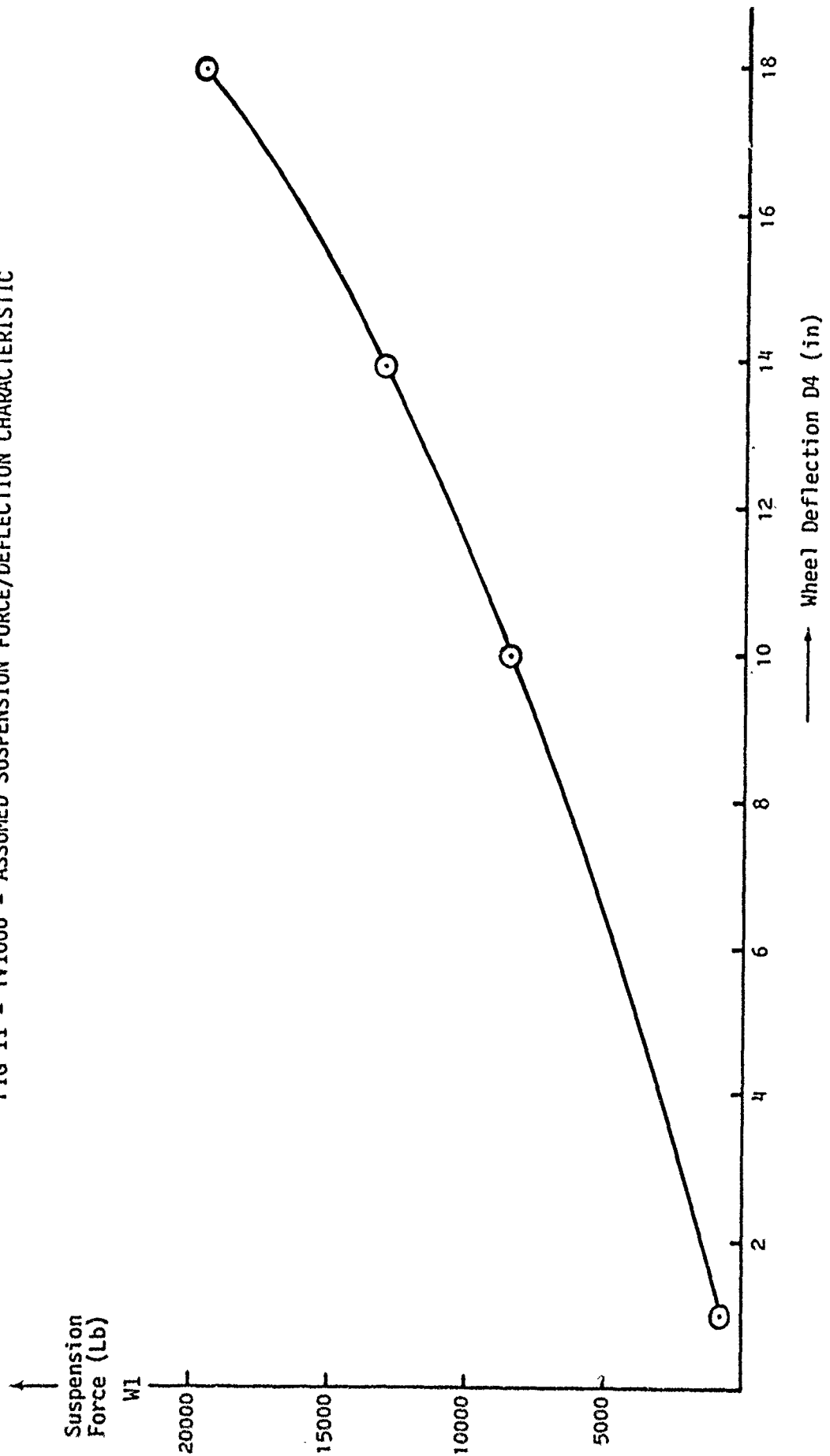


FIG 12 - TV1000 - ESTIMATION OF WHEEL/GROUND CONTACT POINT MOVEMENT

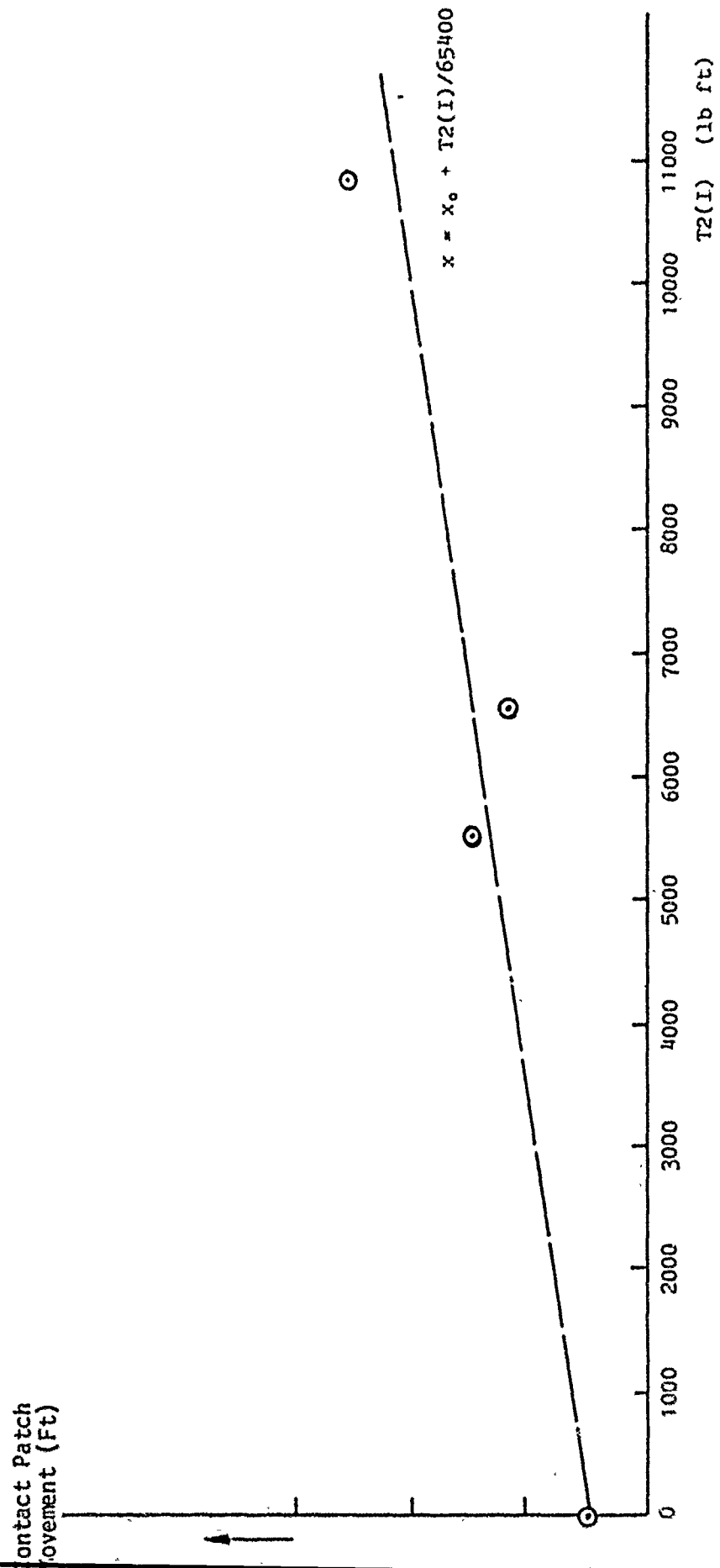
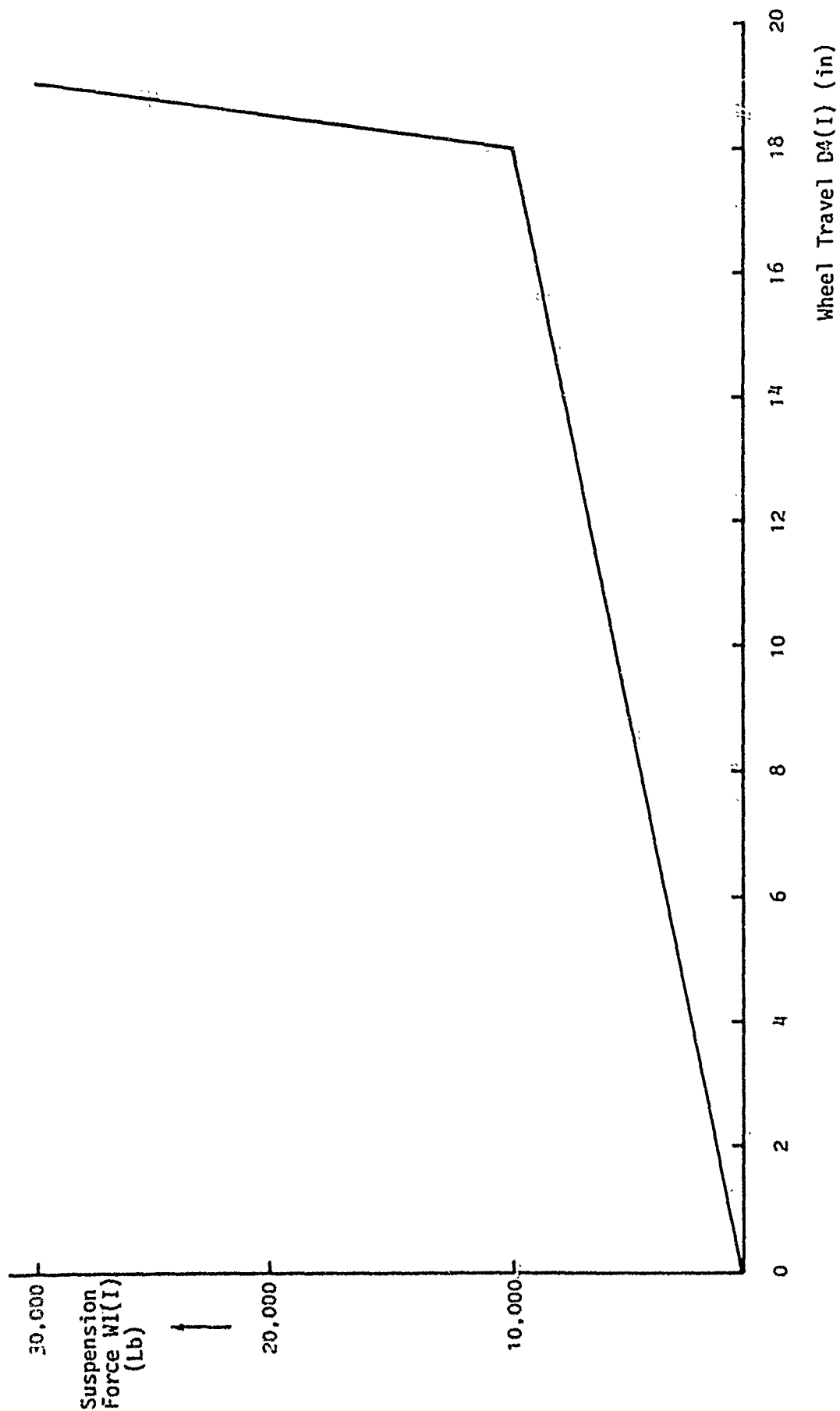
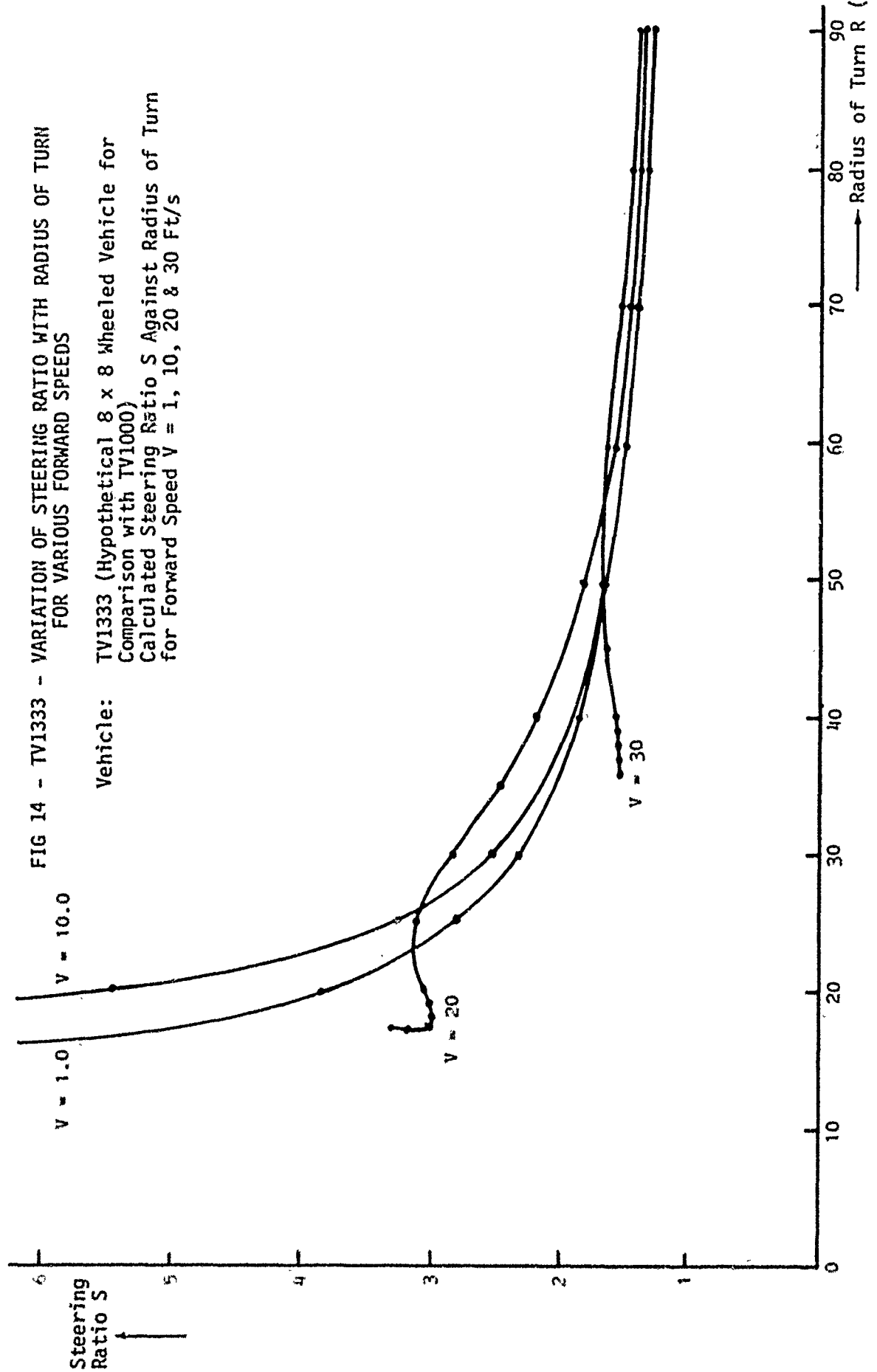


FIG 13 - TV6000TR - ASSUMED SUSPENSION FORCE/DEFLECTION CHARACTERISTIC







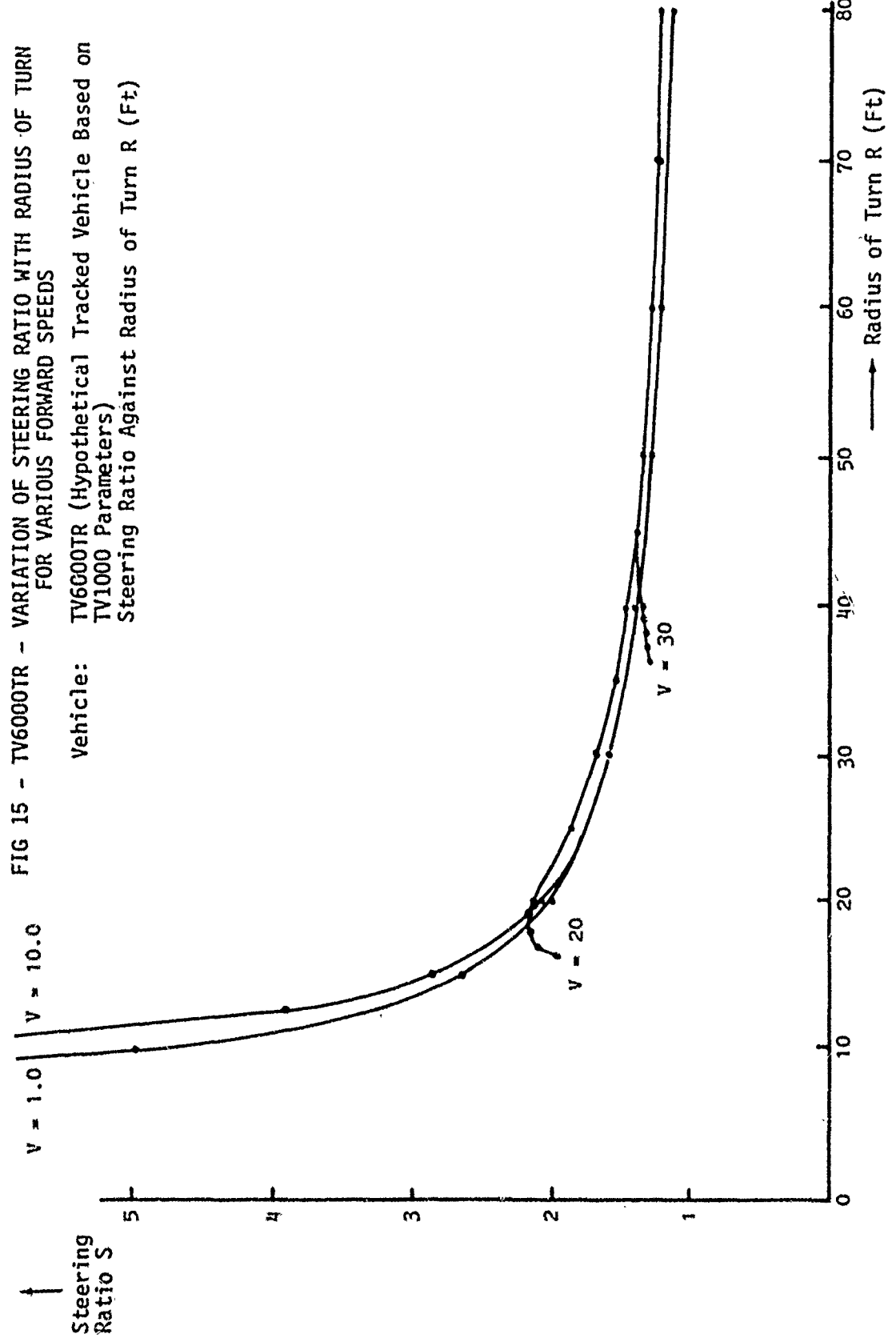
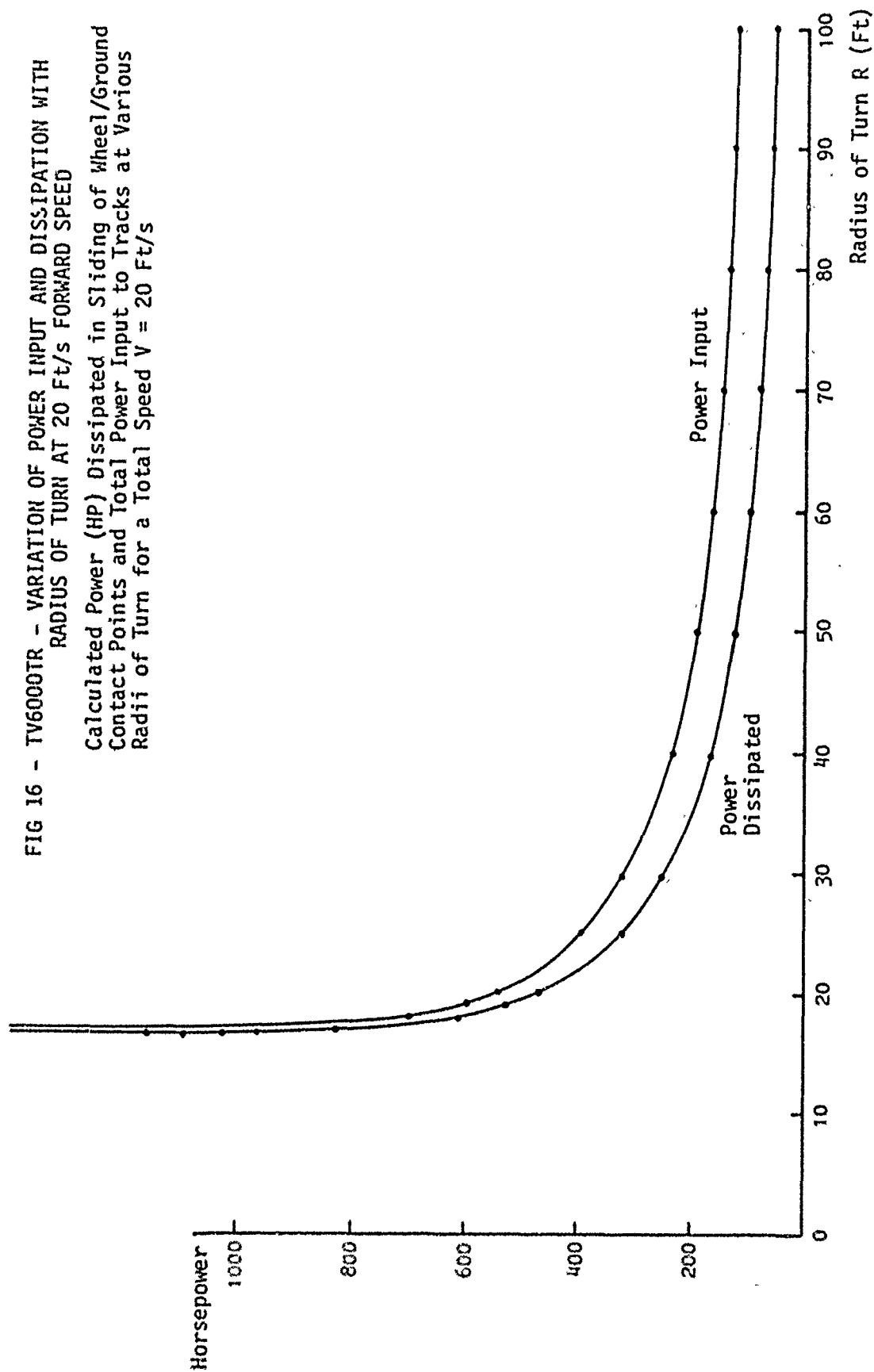
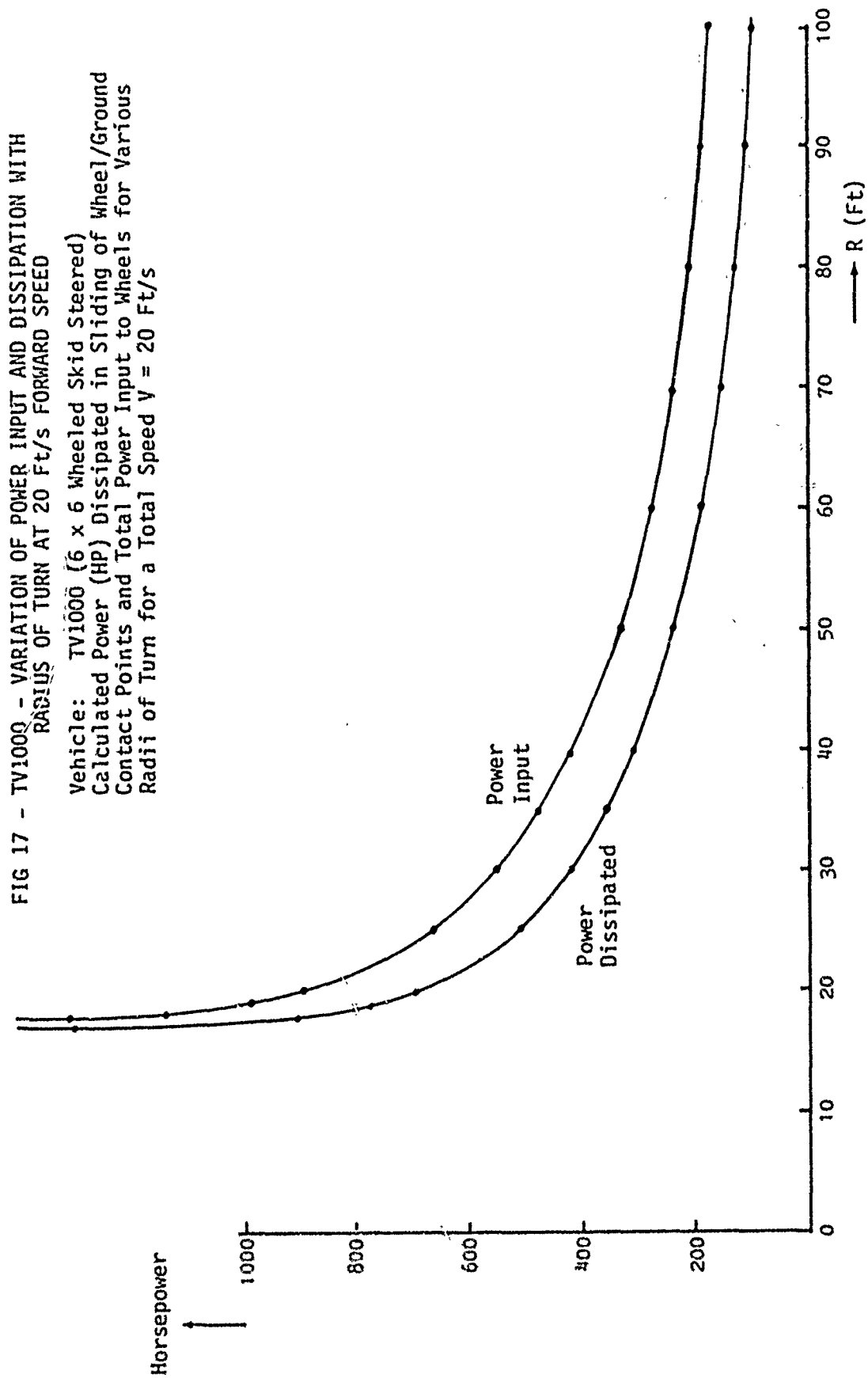


FIG 16 - TV6000TR - VARIATION OF POWER INPUT AND DISSIPATION WITH  
RADIUS OF TURN AT 20 Ft/s FORWARD SPEED  
Calculated Power (HP) Dissipated in Sliding of Wheel/Ground  
Contact Points and Total Power Input to Tracks at Various  
Radii of Turn for a Total Speed  $V = 20$  Ft/s





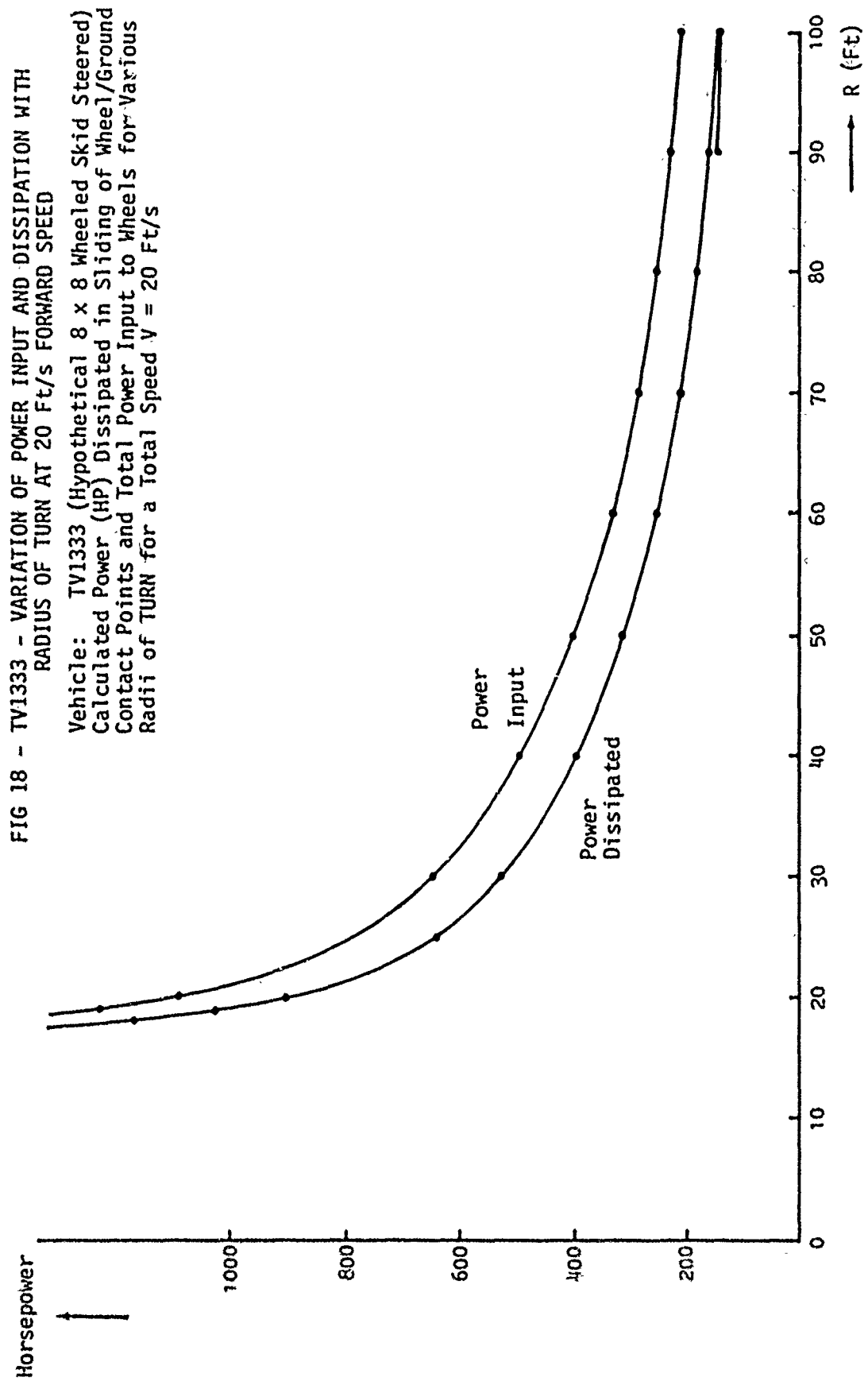


FIG 19 - TV1000 - VARIATION OF SPECIFIC COORDINATES  
OF ICR WITH HEADING ANGLE AT A FIXED SLOPE  
Vehicle: TV1000 (6 x 6 Wheeled Skid Steered)  
Variation of Calculated A(1), A(2), B  
(ICR Coordinates) with Heading Angle G8 on  
a Slope of 38 Degrees  
Positive A(2) Indicates Positive Slip of  
'Inside' Wheels

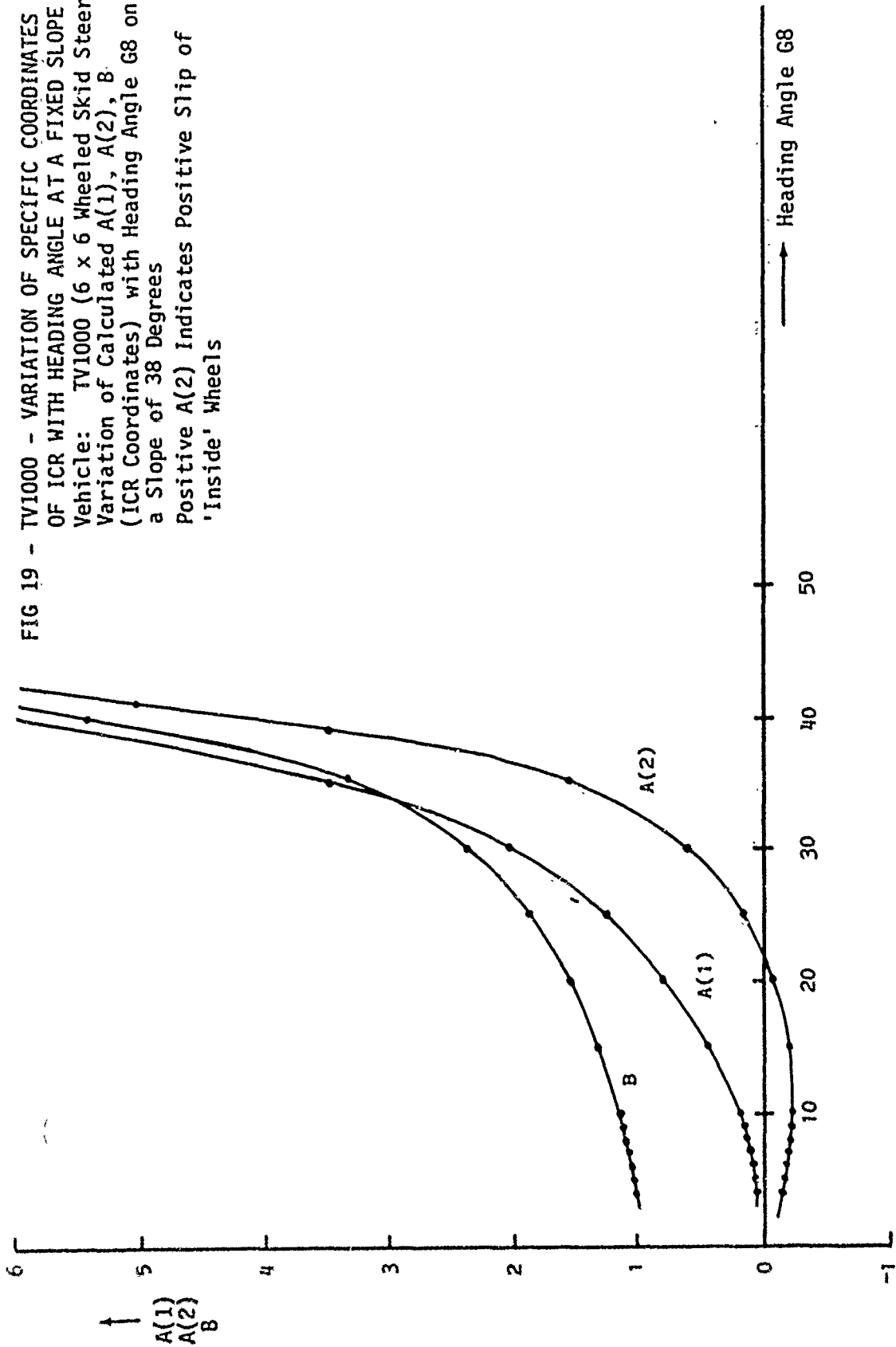


FIG 20 - TV1000 - SLOPE STEERABILITY DIAGRAM

Vehicle: TV1000 (6 x 6 Wheeled Skid Steered)  
 Indicating Boundaries of Slope and Slope Heading Angle  
 for which Solutions were found for Skid Steering  
 Equations, with Negligible Forward Speed. Solid Line  
 Shows Transition from Negative to Positive Slip of  
 'Inside' Wheels.

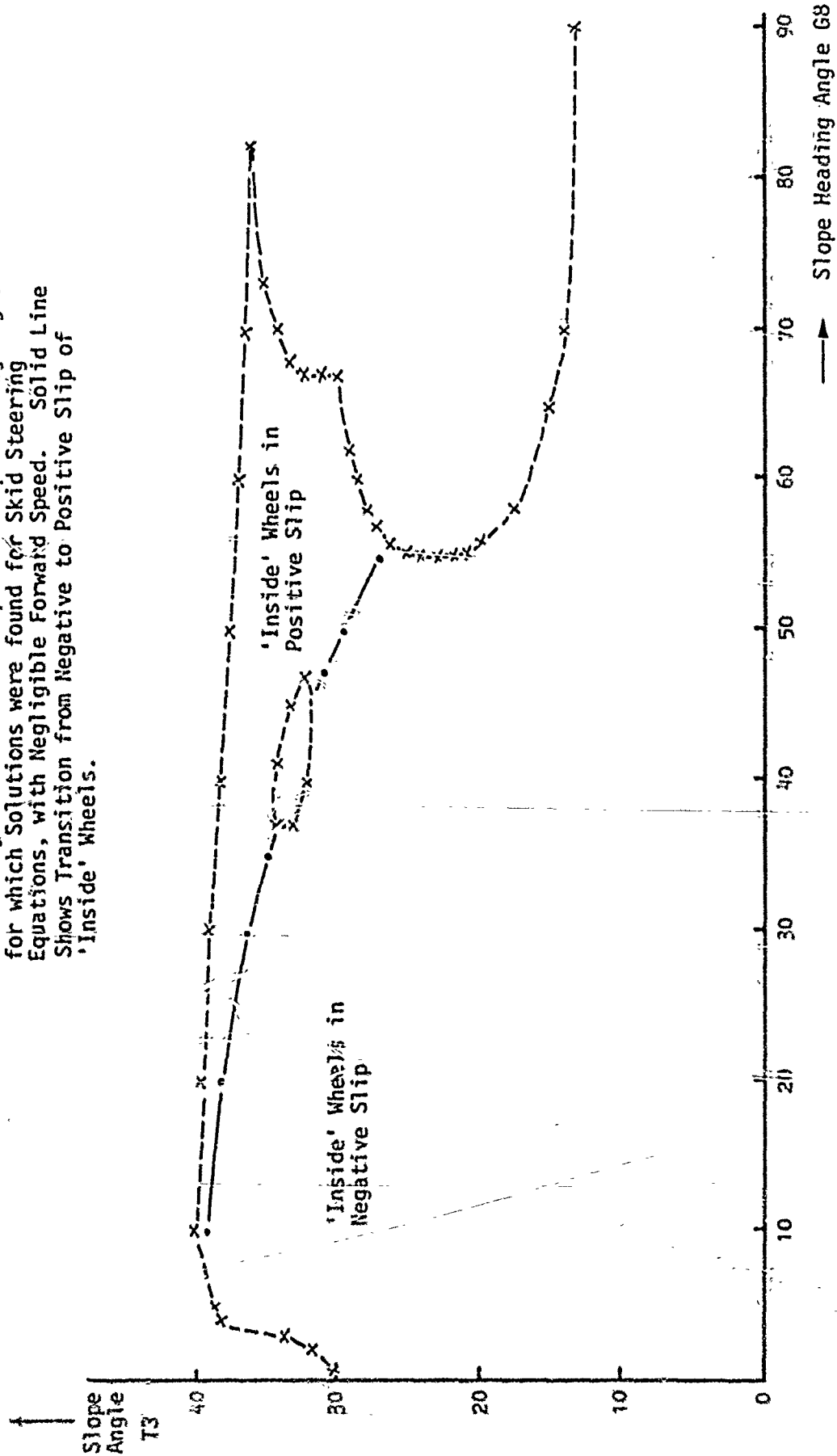


FIG 21 - TV1000 - VARIATION OF STEERING RATIO WITH RADIUS OF TURN  
AT NEGLIGIBLE FORWARD SPEED

Vehicle: TV1000 (6 x 6 Wheeled Skid Steered)  
Variation of Steering Ratio  $S$  Against Radius of Turn  $R$   
at Negligible Total Speed ( $V = \pm 0.1$  Ft/s)

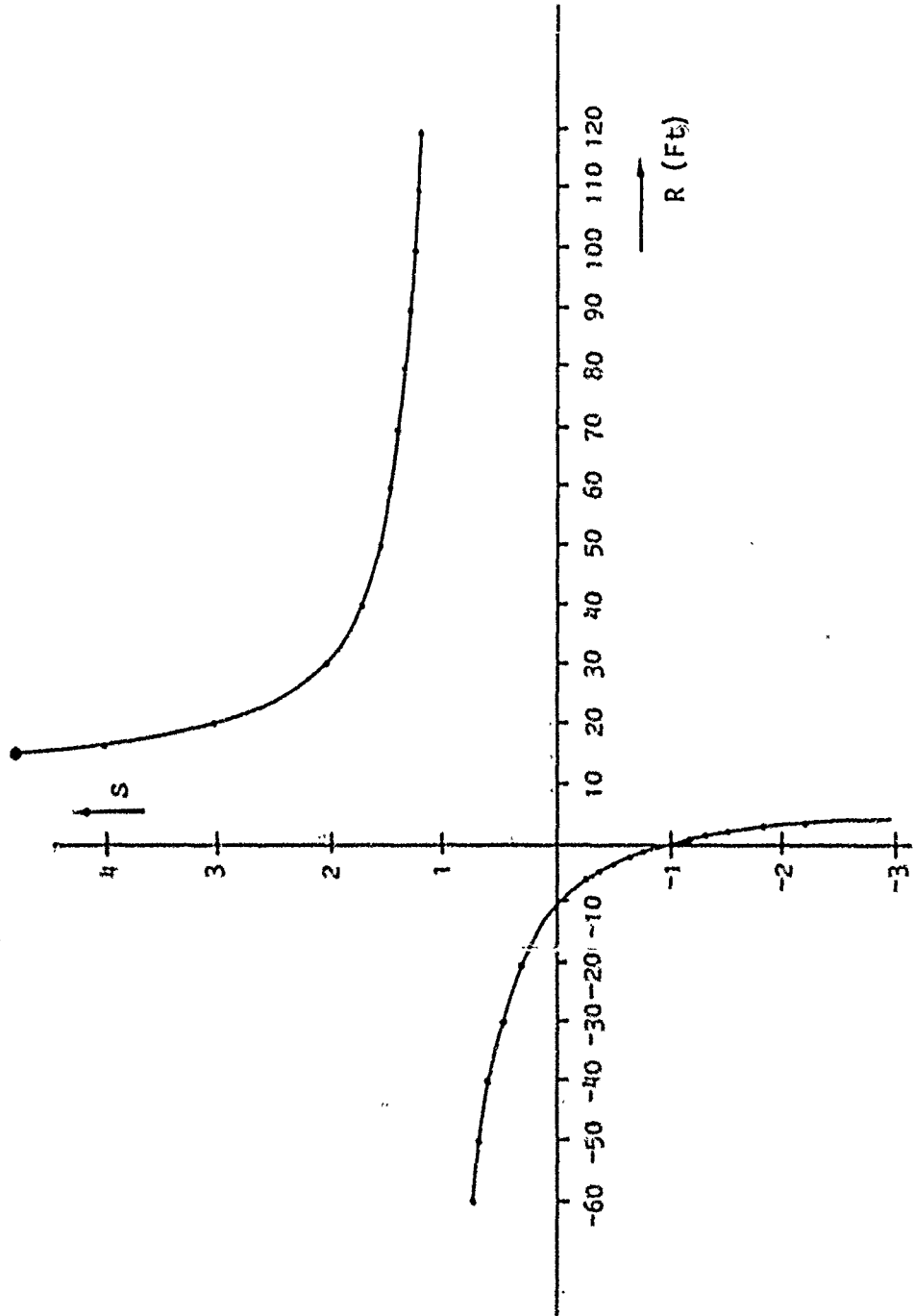


FIG 22 - TV1333 - SLOPE STEERABILITY DIAGRAM

Vehicle: TV1333 (Hypothetical 8 x 8 Wheeled Skid Steered, for Comparison with TV1000)  
 Indicating Boundaries of Slope and Slope Heading Angle for which Solutions were found for Skid Steering Equations, with Negligible Forward Speed.  
 Solid Line shows Transition from Negative to Positive Slip of 'Inside' Wheels.

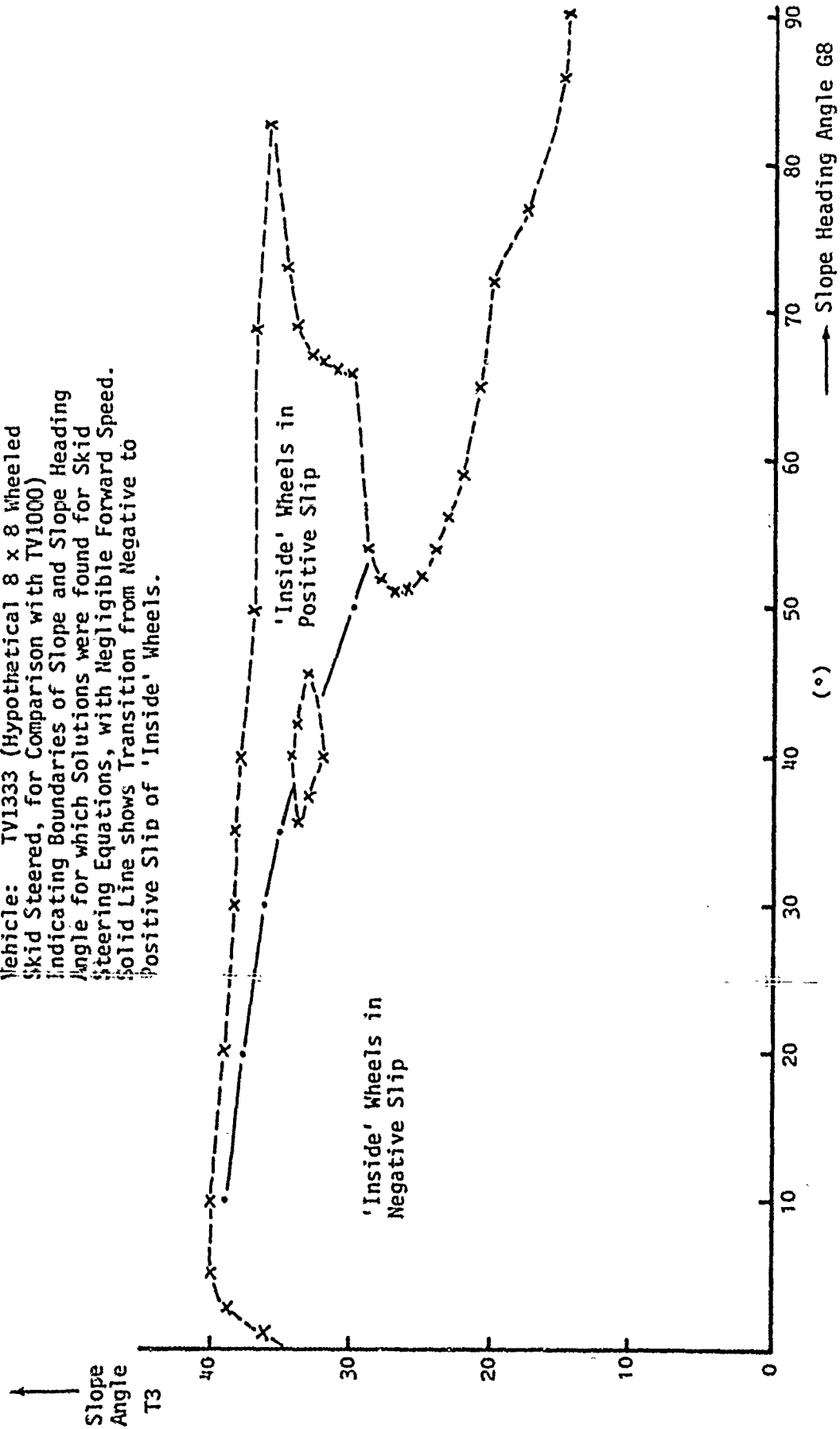




FIG 23 - TV6000TR - SLOPE STEERABILITY DIAGRAM

Vehicle: TV6000TR (Hypothetical Tracked Vehicle based on TV1000 Parameters)  
 Indicating Boundaries of Slope and Slope Heading Angle for which Solutions were found for Skid Steering Equations, with Negligible Forward Speed.  
 Solid Line shows Transition from Negative to Positive Slip of the 'Inside' Track.

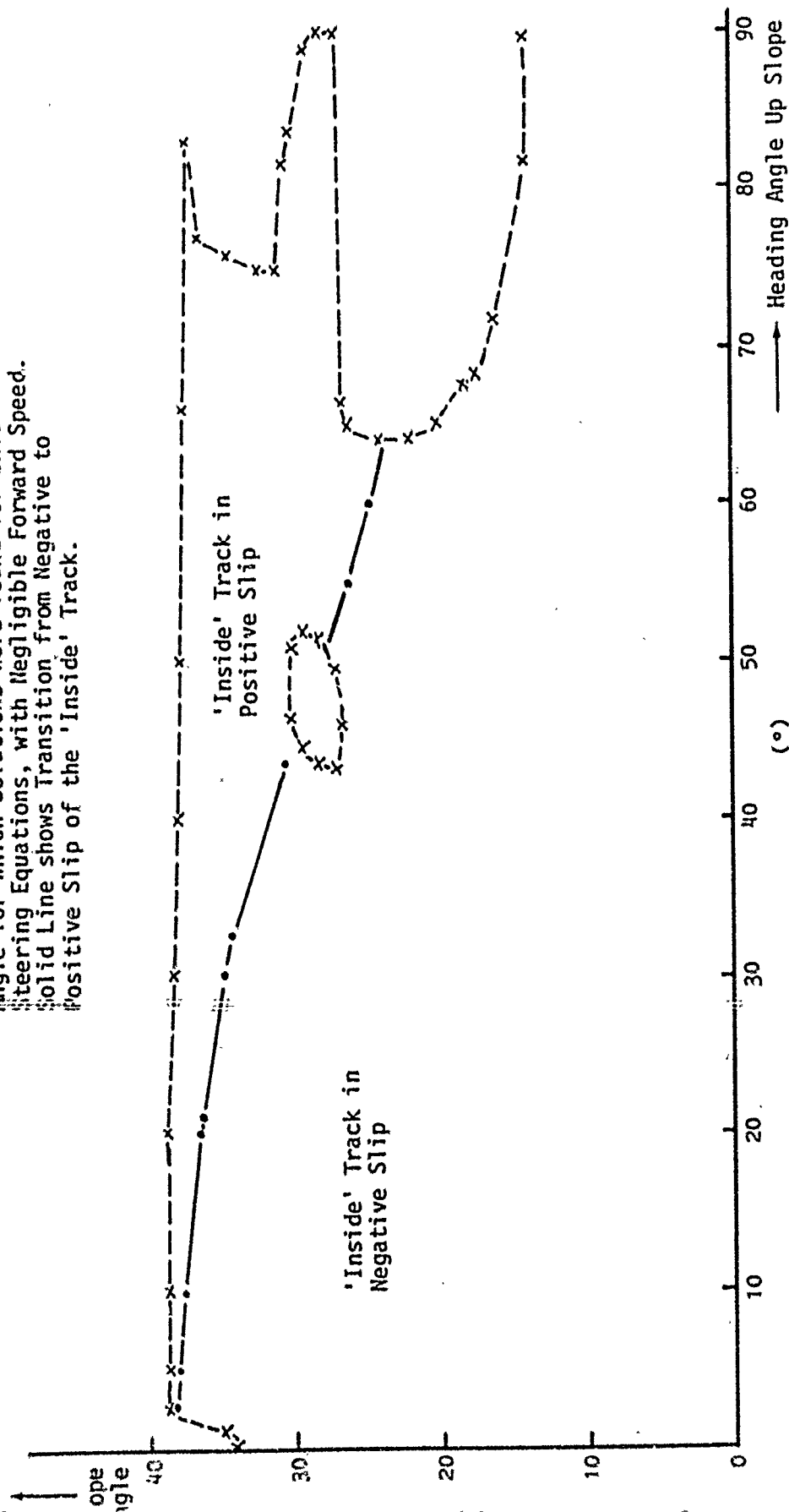
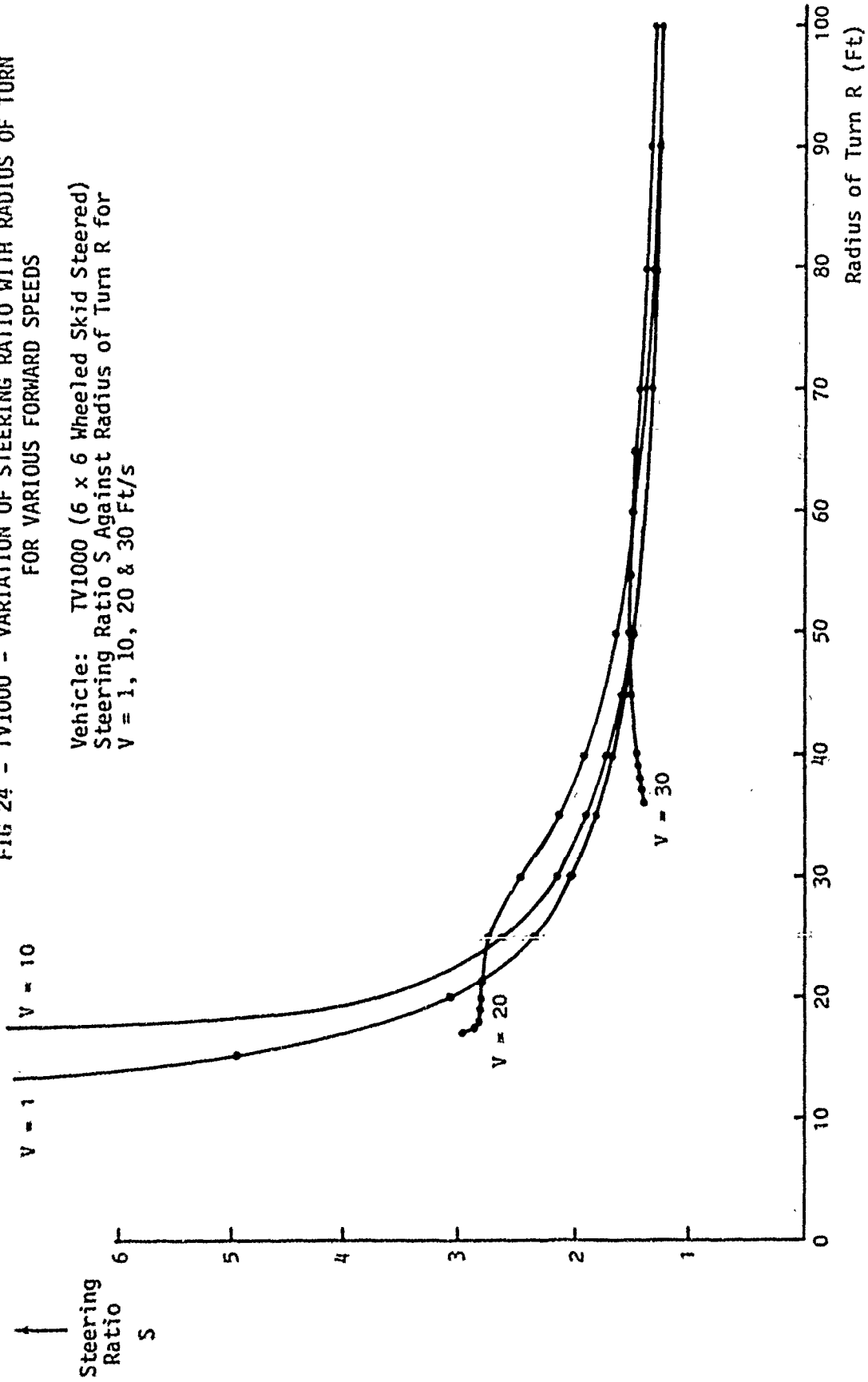


FIG 24 - TV1000 - VARIATION OF STEERING RATIO WITH RADIUS OF TURN  
FOR VARIOUS FORWARD SPEEDS

Vehicle: TV1000 (6 x 6 Wheeled Skid Steered)  
Steering Ratio  $S$  Against Radius of Turn  $R$  for  
 $V = 1, 10, 20 \text{ \& } 30 \text{ Ft/s}$



*D-25*  
DOCUMENT CONTROL DATA SHEET

1.a. AR No 002.715	1.b. Establishment No EDE 38/84	2. Document Date Dec 84	3. Task No MF8001
4. Title SKID STEERING OF WHEELED AND TRACKED VEHICLES - ANALYSIS WITH COULOMB FRICTION ASSUMPTIONS		5. Security a. Document U b. Title U c. Abstract U	6. No of Pages
		7. No of Refs. 4	
8. Author(s) A.P. CREEDY		9. Downgrading Instructions Not Applicable	
10. Corporate Author and Address Engineering Development Establishment Maribyrnong Victoria		11. Authority (as appropriate) a. Sponsor..... EDE b. Security..... EDE c. Downgrading..... EDE d. Approval ..... EDE	
12. Secondary Distribution (of this Document) Approved for Public Release			
13. This document may be ANNOUNCED in catalogues and awareness services available to..... No Limitation			
14. Descriptors Coulomb Friction Steering Steering Gear Tracked Vehicles		15. COSATI Group 1306	
<p>16. Abstract/Summary) Existing theoretical procedures for analysis of skid steering of wheeled and tracked vehicles have been extended to consider the interaction of forces generated for skid steering with the vertical loads carried at each wheel of the vehicle.</p> <p>The developed theory has been organized into a system for numerical calculations of skid steering performance, which has been used to compare the predicted skid steering performance of a 6 x 6 wheeled vehicle, a 8 x 8 wheeled vehicle and a tracked vehicle with 12 road wheels.</p> <p>The results indicated that the wheeled vehicles require greater 'track speed' difference and power input to maintain a steady turn than the tracked vehicle, and that the tracked vehicle can be expected to maintain its ability to steer over a wider range of slope angles and slope heading angles, than the wheeled vehicles. The 8 x 8 wheeled vehicle considered did not appear to offer any significant advantage, in terms of steering performance, over the 6 x 6 vehicle.</p> <p>The results of the slope steerability calculations and, in the case of the 6 x 6 vehicle, comparison of calculated results with experimental data, indicated limitations to the developed theory which require further work to resolve. <i>Additional keywords. charts, Coulomb Friction, Steering gear.</i></p>			